

On the identifiability of Bayesian factor analytic models

Panagiotis Papastamoulis¹ and Ioannis Ntzoufras¹

¹Computational and Bayesian Statistics Lab, Department of Statistics, Athens University of Economics and Business, Athens, Greece e-mail: papastamoulis@aueb.gr ntzoufras@aueb.gr

Abstract: A well known identifiability issue in factor analytic models is the invariance with respect to orthogonal transformations. This problem burdens the inference under a Bayesian setup, where Markov chain Monte Carlo (MCMC) methods are used to generate samples from the posterior distribution. We introduce a post-processing scheme in order to deal with rotation, sign and permutation invariance of the MCMC sample. The exact version of the contributed algorithm requires to solve 2^q assignment problems per (retained) MCMC iteration, where q denotes the number of factors of the fitted model. For large numbers of factors two approximate schemes based on simulated annealing are also discussed. We demonstrate that the proposed method leads to interpretable posterior distributions using synthetic and publicly available data from typical factor analytic models as well as mixtures of factor analyzers. An R package is available online at CRAN web-page.

Keywords and phrases: Bayesian Factor Models, Identifiability, MCMC.

1. Introduction

Factor Analysis (FA) is used to explain relationships among a set of observable responses using latent variables. This is typically achieved by expressing the observed multivariate data as a linear combination of a set of unobserved and uncorrelated variables of considerably lower dimension which are known as factors. Let $Y_i = (Y_{i1}, \dots, Y_{ip})^\top$ denote the i -th observation of a random sample of p dimensional observations with $Y_i \in \mathbb{R}^p$; $i = 1, \dots, n$. Let $\mathcal{N}_p(\mu, \Sigma)$ denotes the p -dimensional normal distribution with mean $\mu = (\mu_1, \dots, \mu_p) \in \mathbb{R}^p$ and covariance matrix Σ and also denote by \mathbf{I}_p the $p \times p$ identity matrix.

In the typical FA model, Y_i is expressed as a linear combination of a latent vector of factors $F_i \in \mathbb{R}^q$

$$Y_i = \mu + \Lambda F_i + \varepsilon_i, \quad i = 1, \dots, n \quad (1)$$

where $q > 0$ denotes a fixed constant. The $p \times q$ dimensional matrix $\Lambda = (\lambda_{rj})$ contains the factor loadings, while $\mu = (\mu_1, \dots, \mu_p)$ contains the marginal mean of Y_i . The unobserved vector of factors $F_i = (F_{i1}, \dots, F_{iq})^\top$ lies on a lower dimensional space, that is, $q < p$ and it consists of uncorrelated features

$$F_i \sim \mathcal{N}_q(0_q, \mathbf{I}_q), \quad (2)$$

independent for $i = 1, \dots, n$, where $0_q := (0, \dots, 0)^\top$.

The error terms (commonly referred to as *uniquenesses* or *idiosyncratic variances*) ε_i are independent from F_i , that is, $\text{Cov}(F_{ij}, \varepsilon_{ik}) = 0, \forall j = 1, \dots, q; k = 1, \dots, p$ and normally distributed

$$\varepsilon_i \sim \mathcal{N}_p(0_p, \Sigma) \quad (3)$$

independent for $i = 1, \dots, n$. Furthermore, ε_i is consisting of independent random variables $\varepsilon_{i1}, \dots, \varepsilon_{ip}$, that is,

$$\Sigma = \text{diag}(\sigma_1^2, \dots, \sigma_p^2). \quad (4)$$

The knowledge of the missing data (F_i) implies that the conditional distribution of Y_i has a diagonal covariance matrix

$$Y_i | F_i \sim \mathcal{N}_p(\mu + \Lambda F_i, \Sigma), \quad (5)$$

independent for $i = 1, \dots, n$. The previous assumptions lead to

$$Y_i \sim \mathcal{N}_p(\mu, \Lambda \Lambda^\top + \Sigma), \quad \text{iid for } i = 1, \dots, n. \quad (6)$$

Without loss of generality we can assume that $\mu = 0_p$. According to Equation (6), the covariance matrix of the marginal distribution of Y_i is equal to $\Lambda \Lambda^\top + \Sigma$. Thus, the latent factors are the only source of correlation among the measurements. This is the crucial characteristic of factor analytic models, where they aim to explain high-dimensional dependencies using a set of lower-dimensional uncorrelated factors (Kim and Mueller, 1978; Bartholomew et al., 2011).

There are two sources of identifiability problems regarding the typical FA model in Equations 1–4. The first one concerns identifiability of Σ and the second one concerns identifiability of Λ . Assuming that Σ is identifiable (see Section 2), we are concerned with identifiability of Λ . It is well known that the factor loadings (Λ) in Equation (1) are only identifiable up to orthogonal transformations. This identifiability issue is not of great practical importance within a frequentist context: the likelihood equations are satisfied by an infinity of solutions, all equally good from a statistical perspective (Lawley and Maxwell, 1962).

On the other hand, under a Bayesian setup it complicates the inference procedure, where MCMC methods are applied to generate samples from the posterior distribution $f(\Lambda, \Sigma, F | \mathbf{y})$. Clearly, the invariance property makes the posterior distribution multimodal. Provided that the MCMC algorithm has converged to the target distribution, the MCMC sample will be consecutively switching among the multiple modes of the posterior surface. Despite the fact that this identifiability problem has no bearings on predictive inference or estimation of the covariance matrix in Equation (6), factor interpretation remains challenging because both Λ and $F_i; i = 1, \dots, n$ are not marginally identifiable. Therefore, the standard practice of providing posterior summaries via ergodic means, or reporting Bayesian credible intervals for factor loadings becomes meaningless due to rotation invariance of the MCMC sample.

Typical implementations of the Bayesian paradigm in FA models use inverse gamma prior on the error variances and normal or truncated normal priors on the factor loadings (Arminger and Muthén, 1998; Song and Lee, 2001). In such cases the model is conditionally conjugate and a MCMC sample can be generated by standard Gibbs sampling (Gelfand and Smith, 1990). However, if Λ is not constrained, the posterior

distribution will have multiple modes leading to a loss of parameter identifiability. Consequently, when MCMC methods are used for estimation of the FA model, inference is not straightforward. On the other hand, in standard factor models, certain identifiability constraints induce undesirable properties, such as a priori order dependence in the off-diagonal entries of the covariance matrix (Bhattacharya and Dunson, 2011). Although tailored methods (briefly reviewed in Section 2) for achieving identifiability and for drawing inference on sparse FA models exist (Conti et al., 2014; Mavridis and Ntzoufras, 2014; Ročková and George, 2016), they require extra modelling effort.

In this paper, the problem of posterior identifiability of the typical FA model is addressed without introducing any additional modelling assumptions. This is achieved by suitably post-processing the simulated MCMC sample of factor loadings, provided by the user. It is demonstrated that the proposed method successfully deals with the non-identifiability of the marginal posterior distribution $f(\Lambda|\mathbf{y})$ and leads to interpretable conclusions. The number of factors (q) is considered fixed, nevertheless a by-product of our implementation is that it can help to reveal cases of overfitting, by simply inspecting simultaneous credible regions of factor loadings.

We propose to correct invariance of simulated factor loadings using a two-stage post-processing approach. At first we focus on generic rotation invariance, that is, to achieve a *simple structure* of factor loadings per MCMC iteration. A factor model with simple structure is one where each measurement is related to at most one latent factor (Thurstone, 1934). Varimax rotations (Kaiser, 1958) are used for this task. After this step, all measurements load at most on one factor while the rest of the loadings are small (close to zero). However, the rotated loadings are still not identifiable across the MCMC trace due to *sign* and *permutation* invariance. Sign switching stems from the fact that we can simultaneously switch the signs of F_i and Λ without altering ΛF_i . Permutation invariance (or *column switching*, according to Conti et al. (2014)) is due to the fact that there is no natural ordering of the columns of the factor loading matrix. Thus, factor labels can change as the MCMC sampler progresses. That being said, the second step is to correct invariance due to specific orthogonal transformations which correspond to *signed-permutations* across the MCMC trace.

The rest of the paper is organized as follows. Section 2 presents the identifiability issues of the FA model and briefly discusses related work. Section 3.1 gives some background on rotations and signed-permutations. The contributed method is introduced in Section 3.2. Three approaches for minimizing the underlying objective function are described in Section 3.3. A geometrical illustration on a toy example is given in Section 3.4. Section 4 applies the proposed method using simulated (Section 4.1) and real (Section 4.2) data. Finally, an application to a model-based clustering problem is given in Section 4.3. An Appendix discusses additional applications and computational aspects of our method.

2. Identifiability problems and related approaches

At first we review some well known results that ensure identifiability of Σ (the *uniqueness problem*) and will be explicitly followed in our implementation. Given that there

are q factors, the number of free parameters in the covariance matrix $\boldsymbol{\Lambda}\boldsymbol{\Lambda}^\top + \boldsymbol{\Sigma}$ is equal to $p + pq - \frac{1}{2}q(q - 1)$ (see [Lawley and Maxwell, 1962](#)). The number of free parameters in the unconstrained covariance matrix of Y_i is equal to $\frac{1}{2}p(p + 1)$. Hence, under the typical FA model, the number of parameters in the covariance matrix is reduced by

$$\frac{1}{2}p(p + 1) - \left[p + pq - \frac{1}{2}q(q - 1) \right] = \frac{1}{2}[(p - q)^2 - (p + q)].$$

The last expression is positive if $q < \phi(p)$ where $\phi(p) := \frac{2p+1-\sqrt{8p+1}}{2}$, a quantity which is known as the Ledermann bound ([Ledermann, 1937](#)). When $q < \phi(p)$ it can be shown that $\boldsymbol{\Sigma}$ is almost surely unique ([Bekker and ten Berge, 1997](#)). We assume that the number of latent factors does not exceed $\phi(p)$.

Given identifiability of $\boldsymbol{\Sigma}$, a second source of identifiability problems is related to orthogonal transformations of the matrix of factor loadings, which is the main focus of this paper. A square matrix \mathbf{R} is an *orthogonal* (or *rotation*) matrix if and only if $\mathbf{R}^\top = \mathbf{R}^{-1}$, that is, its inverse equals to its transpose. Consider a $q \times q$ orthogonal matrix \mathbf{R} and define $\tilde{F}_i = \mathbf{R}F_i$. It follows that the representation $Y_i = \mu + \boldsymbol{\Lambda}\mathbf{R}^\top \tilde{F}_i + \varepsilon_i$ leads to the same marginal distribution of Y_i as the one in Equation (6). Since the likelihood is invariant under orthogonal transformations, the posterior distribution will typically exhibit many modes under vaguely informative prior distributions.

A popular technique ([Geweke and Zhou, 1996](#); [Fokoué and Titterington, 2003](#); [West, 2003](#); [Lopes and West, 2004](#); [Lucas et al., 2006](#); [Carvalho et al., 2008](#); [Mavridis and Ntzoufras, 2014](#); [Papastamoulis, 2018, 2020](#)) in order to deal with rotational invariance in Bayesian FA models relies on a lower-triangular expansion of $\boldsymbol{\Lambda}$, first suggested by [Anderson and Rubin \(1956\)](#), that is:

$$\boldsymbol{\Lambda} = \begin{pmatrix} \lambda_{11} & 0 & \cdots & 0 \\ \lambda_{21} & \lambda_{22} & \cdots & 0 \\ \vdots & \vdots & \ddots & \vdots \\ \lambda_{q1} & \lambda_{q2} & \cdots & \lambda_{qq} \\ \vdots & \vdots & \ddots & \vdots \\ \lambda_{p1} & \lambda_{p2} & \cdots & \lambda_{pq} \end{pmatrix}. \quad (7)$$

However this approach still fails to correct the invariance due to sign-switching across the MCMC trace; see, for example, at Figure 2.(b) in [Papastamoulis \(2018\)](#). Additional constraints are introduced for addressing this issue, e.g. by assuming that the diagonal elements are strictly positive ([Aguilar and West, 2000](#)). Besides the upper triangle of the loading matrix that is fixed to zero a-priori, the remaining elements in the lower part of the matrix are also allowed to take values in areas close to zero (e.g. this is the case when the first variable does not load on any factor). In such a case, identifiability of $\boldsymbol{\Lambda}$ is lost; see Theorem 5.4 in [Anderson and Rubin \(1956\)](#). Of course this problem can be alleviated by suitably reordering the variables, however the choice of the first q response variables is crucial ([Carvalho et al., 2008](#)).

[Conti et al. \(2014\)](#) augment the FA model with a binary matrix, indicating the latent factor on which each variable loads. They also consider an extension of the model

by also allowing correlation among factors. Under suitable identification criteria, a prior distribution restricts the MCMC sampler to explore regions of the parameter space corresponding to models which are identified up to column and sign switching. Then, they deal with sign and column switching by using simple reordering heuristics which are driven by the existence of zeroes in their loading matrix. At each MCMC iteration, the non-zero columns are reordered such that the top elements appear in increasing order. Next, sign-switching is treated by using a benchmark factor loading (e.g., the factor loading with the highest posterior probability of being different from zero in each column) in each column and then switching the signs at each MCMC iterations in order to agree with the benchmark.

[Mavridis and Ntzoufras \(2014\)](#) place a normal mixture prior on each element of Λ and introduce an additional set of latent binary indicators which is used to identify whether an item is associated with the corresponding factor. They also reorder the items such that important non-zero loadings are placed in the diagonal of Λ in Equation (7). [Ročková and George \(2016\)](#) identify the FA model by expanding the parameter space using an auxiliary parameter matrix which drives the implied rotation. The whole procedure is fully model driven and it is implemented through-an Expectation-Maximization type algorithm. Additionally, the varimax rotation is suggested every few iterations of the algorithm to stabilize and speed up the convergence of the algorithm.

3. Method

3.1. Notation and definitions

Denote as \mathcal{T}_q the set of all permutations of $\{1, \dots, q\}$. Each permutation $\nu \in \mathcal{T}_q$ corresponds to a $q \times q$ *permutation matrix* \mathbf{P} , which is a square binary matrix that has exactly one 1 in each row and each column and 0 elsewhere. For example, consider the permutation $\nu = (3, 1, 2) \in \mathcal{T}_3$ which corresponds to the 3×3 permutation matrix

$$\mathbf{P} = \begin{pmatrix} 0 & 0 & 1 \\ 1 & 0 & 0 \\ 0 & 1 & 0 \end{pmatrix}.$$

A *signed permutation matrix* is a square matrix which has precisely one nonzero entry in every row and column and whose only nonzero entries are 1 and/or -1 (see e.g. [Snapper, 1979](#)). A $q \times q$ signed permutation matrix \mathbf{Q} can be expressed as

$$\mathbf{Q} = \mathbf{SP}, \tag{8}$$

where \mathbf{P} is a $q \times q$ permutation matrix and $\mathbf{S} = \text{diag}(s_1, \dots, s_q)$ is a $q \times q$ diagonal matrix with diagonal entries equal to $s_j \in \{-1, 1\}$, $j = 1, \dots, q$. For example, consider that

$$\mathbf{Q} = \begin{pmatrix} 0 & 0 & -1 \\ -1 & 0 & 0 \\ 0 & 1 & 0 \end{pmatrix} = \begin{pmatrix} -1 & 0 & 0 \\ 0 & -1 & 0 \\ 0 & 0 & 1 \end{pmatrix} \begin{pmatrix} 0 & 0 & 1 \\ 1 & 0 & 0 \\ 0 & 1 & 0 \end{pmatrix}.$$

It is evident that applying a signed permutation \mathbf{Q} to a $p \times q$ matrix $\mathbf{\Lambda}$ results to the transformed matrix arising from the corresponding signed permutation of its columns. For example

$$\mathbf{\Lambda} \mathbf{Q} = \mathbf{\Lambda} \mathbf{S} \mathbf{P} = \begin{pmatrix} \lambda_{11} & \lambda_{12} & \lambda_{13} \\ \vdots & \vdots & \vdots \\ \lambda_{p1} & \lambda_{p2} & \lambda_{p3} \end{pmatrix} \begin{pmatrix} 0 & 0 & -1 \\ -1 & 0 & 0 \\ 0 & 1 & 0 \end{pmatrix} = \begin{pmatrix} -\lambda_{12} & \lambda_{13} & -\lambda_{11} \\ \vdots & \vdots & \vdots \\ -\lambda_{p2} & \lambda_{p3} & -\lambda_{p1} \end{pmatrix}$$

is generated by first switching the signs of the first two columns and then permuting according to $\nu = (3, 1, 2)$.

A permutation matrix is a special case of a rotation (or orthogonal) matrix. The rotation is proper if $\det(\mathbf{R}) = 1$. Permutation matrices represent proper rotations. In case that $\det(\mathbf{R}) = -1$, the rotation is improper. Signed permutation matrices are a subgroup of improper rotation matrices.

3.2. Rotation-Sign-Permutation post processing algorithm

Given a $p \times q$ matrix $\mathbf{\Lambda}$ of factor loadings, the varimax problem (Kaiser, 1958) is to find a $q \times q$ rotation matrix $\mathbf{\Phi}$ such that the sum of the within-factor variances of squared factor loadings of the rotated matrix of loadings $\tilde{\mathbf{\Lambda}} = \mathbf{\Lambda} \mathbf{\Phi}$ is maximized. That is, the optimization problem is now summarized by

$$\begin{aligned} \text{maximize} \quad & \frac{1}{4} \sum_{j=1}^q \left[\left(\sum_{r=1}^p \tilde{\lambda}_{rj}^4 \right) - \frac{1}{p} \left(\sum_{r=1}^p \tilde{\lambda}_{rj}^2 \right)^2 \right] \\ \text{subject to} \quad & \mathbf{\Phi}^\top \mathbf{\Phi} = \mathbf{I}_q \\ \text{where} \quad & \tilde{\lambda}_{rj} = \sum_{k=1}^q \lambda_{rk} \phi_{kj}, \quad r = 1, \dots, p; \quad j = 1, \dots, q. \end{aligned} \quad (9)$$

The original approach for solving the varimax problem was to increase the objective function by successively rotating pairs of factors (Kaiser, 1958). Subsequent developments based on matrix formulations of the varimax problem involved the simultaneous rotation of all factors to improve the objective function (Sherin, 1966; Neudecker, 1981; ten Berge, 1984).

We used the `varimax()` base function in R to solve the varimax problem. So assuming that we have at hand a simulated output of factor loadings $\mathbf{\Lambda}^{(t)}$, $\mathbf{\Lambda}^{(t)} = (\lambda_{rj}^{(t)})$, $t = 1, \dots, T$, we denote as $\tilde{\mathbf{\Lambda}}^{(t)} = (\tilde{\lambda}_{rj}^{(t)})$, $t = 1, \dots, T$ the rotated MCMC output, after solving the varimax problem per MCMC iteration, where T is the size of MCMC iterations.

After solving the varimax problem for each MCMC iteration, the second stage of our solution is to apply signed permutations to the MCMC output until the transformed loadings are sufficiently close to a reference value denoted as $\mathbf{\Lambda}^*$. For instance we will assume that $\mathbf{\Lambda}^*$ corresponds to a fixed matrix, however we will relax this

assumption later. Let \mathcal{Q}_q denotes the set of $q \times q$ signed permutation matrices. The optimization problem is stated as

$$\begin{aligned} & \text{minimize} \quad \sum_{t=1}^T \|\tilde{\Lambda}^{(t)} \mathbf{Q}^{(t)} - \Lambda^*\|^2 \\ & \text{subject to} \quad \mathbf{Q}^{(t)} \in \mathcal{Q}_q, \quad t = 1, \dots, m, \end{aligned} \quad (10)$$

where $\|\mathbf{A}\| = \sqrt{\sum_i \sum_j \alpha_{ij}^2}$ denotes the Frobenious norm on the matrix space. By Equation (8), it follows that

$$\|\tilde{\Lambda} \mathbf{Q} - \Lambda^*\|^2 = \|\tilde{\Lambda} \mathbf{S} \mathbf{P} - \Lambda^*\|^2 = \sum_{r=1}^p \sum_{j=1}^q \left(s_j \tilde{\lambda}_{r\nu_j} - \lambda_{rj}^* \right)^2,$$

where $\nu = (\nu_1, \dots, \nu_q) \in \mathcal{T}_q$ denotes the permutation vector corresponding to the permutation matrix \mathbf{P} and \mathcal{T}_q denotes the set of all permutations of $\{1, \dots, q\}$. Thus, (10) can be also written as

$$\begin{aligned} & \text{minimize} \quad \sum_{t=1}^T \sum_{r=1}^p \sum_{j=1}^q \left(s_j^{(t)} \tilde{\lambda}_{r\nu_j^{(t)}} - \lambda_{rj}^* \right)^2 \end{aligned} \quad (11)$$

$$\text{subject to} \quad s_j^{(t)} \in \{-1, 1\}, \quad t = 1, \dots, m; j = 1, \dots, q \quad (12)$$

$$\text{and} \quad \nu^{(t)} \in \mathcal{T}_q, \quad t = 1, \dots, m. \quad (13)$$

Clearly, the reference loading matrix $\Lambda^* = (\lambda_{rj}^*)$ is not known, thus it is approximated by a recursive algorithm. This approach is inspired by ideas used for solving identifiability problems in the context of Bayesian analysis of mixture models (Stephens, 2000; Papastamoulis and Iliopoulos, 2010; Rodriguez and Walker, 2014), known as *label switching* (see Papastamoulis, 2016, for a recent review of these methods).

The proposed Varimax Rotation-Sign-Permutation (RSP) post processing algorithm aims to select Λ^*, s, ν such that we

$$\text{minimize} \quad \Psi(\Lambda^*, s, \nu) = \sum_{t=1}^T \sum_{r=1}^p \sum_{j=1}^q \left(s_j \tilde{\lambda}_{r\nu_j^{(t)}} - \lambda_{rj}^* \right)^2. \quad (14)$$

The algorithm is composed by two main steps implemented iteratively: the first minimizes $\Psi(\Lambda^*, s, \nu)$ with respect to Λ^* for given values of (s, ν) (Reference-Loading Matrix Estimation, RLME, step), while the second, with respect to (s, ν) for given value of Λ^* (RSP step); see Algorithm 1 for a concise summary.

For Step 2.2.1, it is straightforward to show that the minimization of $\Psi(\Lambda^*, s, \nu)$ with respect to Λ^* for given values of (s, ν) is obtained by

$$\lambda_{rj}^* = \frac{1}{T} \sum_{t=1}^T s_j^{(t)} \tilde{\lambda}_{r\nu_j^{(t)}}^{(t)},$$

Algorithm 1: Varimax-RSP algorithm (Correcting rotation, sign and permutation invariance to a MCMC sample of factor loadings)

Input : Simulated MCMC sample of factor loadings $\{\Lambda^{(t)}, t = 1, \dots, T\}$.
Output: Reordered MCMC sample of factor loadings $\{\tilde{\Lambda}^{(t)}, t = 1, \dots, T\}$.

Step 1: Varimax Rotation Step

```

for  $t = 1$  to  $T$ 
  | Implement the varimax rotation on  $\Lambda^{(t)}$  by solving (9) and obtain the rotated varimax
  | loadings  $\tilde{\Lambda}^{(t)}$ .
endfor

```

Step 2: Signed Permutation Step

Step 2.1 Initialization:

```

for all  $t \in \{1, \dots, T\}$ : Initialize  $s^{(t)}$  and  $\nu^{(t)}$ ;
Proposed initialization
  | for all  $t \in \{1, \dots, T\}$  and  $j \in \{1, \dots, q\}$ : Set  $s_j^{(t)} = 1$  and  $\nu_j^{(t)} = j$  (identity
  | permutation);
end

```

Step 2.2

```

repeat
  | Step 2.2.1 RLME step
    | Set
      |  $\lambda_{rj}^* = \frac{1}{T} \sum_{t=1}^T s_j^{(t)} \tilde{\lambda}_{r\nu_j^{(t)}}^{(t)}, \quad r = 1, \dots, p; j = 1, \dots, q$ 
      | where  $\tilde{\lambda}_{rj}^{(t)}$  are the varimax rotated loadings.
  | Step 2.2.2 SP step
    | for each iteration  $t = 1, \dots, T$ 
      | Solve the problem
        |  $(s^{(t)}, \nu^{(t)}) = \operatorname{argmin}_{s, \nu} \left\{ \mathcal{L}_{s, \nu}^{(t)} : s \in \{-1, 1\}^q, \nu \in \mathcal{T}_q \right\}, \quad (15)$ 
        | where
        | 
$$\mathcal{L}_{s, \nu}^{(t)} := \sum_{r=1}^p \sum_{j=1}^q \left( s_j \tilde{\lambda}_{r\nu_j^{(t)}}^{(t)} - \lambda_{rj}^* \right)^2.$$

    | endfor
  | until no improvement in  $\Psi(\Lambda^*, s, \nu) = \sum_{t=1}^T \mathcal{L}_{s^{(t)}, \nu^{(t)}}^{(t)}$  is observed;

```

END of algorithm.

for $r = 1, \dots, p$, $j = 1, \dots, q$. Step 2.2.2 is composed by the Sign-Permutation (SP) step which minimizes $\Psi(\Lambda^*, s, \nu)$ with respect to (s, ν) for a given reference loading matrix Λ^* . Step 2 can also serve as a stand alone algorithm, that is, without the varimax rotation step (an application is given in Appendix A, for the problem of comparing multiple MCMC chains). Alternative strategies for minimizing expression (15), are provided in Section 3.3 which follows.

3.3. Computational Strategies for the Sign-Permutation (SP) step

The optimal solution of (15) can be found exactly by solving the assignment problem (see Burkard et al., 2009) using a full enumeration of the total 2^q combinations $s^{(t)} \in \{-1, 1\}^q$. Although this computational strategy avoids the evaluation of the objective function for all $2^q q!$ feasible solutions, it still requires to solve 2^q assignment problems. Thus, for models with many factors (say $q > 10$) we propose an approximate algorithm based on simulated annealing (Kirkpatrick et al., 1983) with two alternative proposal distributions.

For typical cases of factor models (e.g. $q \leq 10$), the minimization in (15) can be performed exactly within reasonable computing time, by performing the following two-step procedure:

- first compute $\min_{\nu \in \mathcal{T}_q} \left\{ \mathcal{L}_{s, \nu}^{(t)} \right\}$, for each of the 2^q possible sign configurations s , and then
- find the (s, ν) that correspond to the overall minimum. The first minimization requires to solve a special version of the transportation problem, known as the assignment problem (see Burkard et al., 2009).

For a given sign matrix $S = \text{diag}(s_1, \dots, s_q) \in \mathcal{S}$, the minimization problem is stated as the assignment problem

$$\begin{aligned} \min_{\delta_{ij} \in \{0,1\}, i, j = 1, \dots, q} \quad & \sum_{i=1}^q \sum_{j=1}^q \delta_{ij} c_{ij} \\ \text{subject to} \quad & \sum_{i=1}^q \delta_{ij} = 1, \quad \forall j = 1, \dots, q \\ & \sum_{j=1}^q \delta_{ij} = 1, \quad \forall i = 1, \dots, q \end{aligned} \tag{16}$$

where the $q \times q$ cost matrix $C = (c_{ij})$ of the assignment problem is defined as

$$c_{ij} = \sum_{r=1}^p \left(s_j \tilde{\lambda}_{rj} - \lambda_{ri}^* \right)^2, \quad i, j = 1, \dots, q$$

and the binary decision variables δ_{ij} are defined as

$$\delta_{ij} := \begin{cases} 1, & \text{if index } i \text{ is assigned to index } j \\ 0, & \text{otherwise} \end{cases}, \quad i, j = 1, \dots, q.$$

We used the library `lpSolve` (Berkelaar et al., 2013) in R in order to solve the assignment problem (16).

Algorithm 2: Sign-Permutation (SP) Step – Exact Scheme (Scheme A)

```

Step A.1
  for each  $s = (s_1, \dots, s_q) \in \{-1, 1\}^q$ 
    | Find the permutation  $\nu(s)$  that minimizes  $\{\mathcal{L}_{s,\nu}^{(t)} : \nu \in \mathcal{T}_q\}$  by solving the assignment
    | problem (16).
  endfor

Step A.2
  | Set  $(s^{(t)}, \nu^{(t)}) = \operatorname{argmin}_{s,\nu} \{\mathcal{L}_{s,\nu}^{(t)} : s \in \{-1, 1\}^q\}$ .

```

END of SP Step.

The exact SP approach is summarized in Algorithm 2. This scheme is elaborate and requires the evaluation of the problem over all possible sign combinations. More specifically, it requires to solve 2^q assignment problems in order to find the overall minimum. As we have already mentioned, this approach is more efficient than a brute force algorithm that requires $2^q q!$ evaluations of the objective function. It can be applied in a reasonable way for models with $q \leq 10$ factors but its implementation becomes forbidden in terms of computational time for models with factors of higher dimension. For this reason, for models with large number of factors, we also propose strategies based on simulated annealing (Kirkpatrick et al., 1983).

Under the Simulated Annealing (SA) framework, *candidate states* (s^*, ν^*) are proposed. The proposal is either accepted as the next state or rejected and the previous state is repeated. This procedure is repeated B times, by gradually cooling down the temperature T_b which controls the acceptance probability at iteration $b = 1, \dots, B$. These annealing steps are implemented for each MCMC iteration t , within step 2.2.2 of Algorithm 1. In the following, two different versions of the SA approach (named “full” and “partial”) are introduced and described in detail.

In the first version of SA scheme (Scheme B: *full SA*), the pair (s^*, ν^*) is generated independently by random switching one element of the current sign vector s and permuting two randomly selected indexes in ν . This scheme is referred to as *full* simulated annealing. It is the simplest approach that can be used to generate candidate states. For this reason, it is expected to be trapped to inferior solutions in some cases.

The second version of SA (Scheme C: *partial SA*) attempts to overcome this problem. It is a hybrid between the exact SA approach (Scheme A) and the full SA (Scheme B). Therefore, it is more sophisticated than full SA but computationally more demanding. Firstly, we propose a candidate sign configuration s^* using a random perturbation of the current value as in Scheme B. Next, we proceed as in the exact approach (Scheme A), by deterministically identifying the permutation ν^* which minimizes $\{\mathcal{L}_{s^*,\nu}^{(t)} : \nu \in \mathcal{T}_q\}$, given s^* . We refer to this scheme as *partial* simulated annealing in order to emphasize that while s^* is randomly generated from the current state, ν^* is deterministically defined given s^* .

Algorithm 3: Sign-Permutation (SP) Step – Simulated Annealing (SA) schemes
 (Scheme B and C)

```

Step 1: Initialize
  Set initial values  $(s^{(t,0)}, \nu^{(t,0)}) = (s^{(t)}, \nu^{(t)})$  and let  $\mathcal{L}^{(t,0)} = \mathcal{L}_{s^{(t)}, \nu^{(t)}}^{(t)}$ .

Step 2
  for  $b = 1$  to  $B$ 
    (a) Propose a candidate state  $(s^*, \nu^*)$  using one of the following schemes:
      SA version 1: Full SA (Scheme B)
        Randomly switch the sign of one index in  $s^{(t,b-1)}$ , and
        Permute the values of a randomly selected pair of indices in  $\nu^{(t,b-1)}$ .
      End-Full-SA
      SA version 2: Partial SA (Scheme C)
        Obtain  $s^*$  by randomly switching the sign of one index in  $s^{(t,b-1)}$ .
        Obtain the permutation  $\nu^* := \nu(s^*)$  that minimizes  $\{\mathcal{L}_{s^*, \nu}^{(t)} : \nu \in \mathcal{T}_q\}$  by solving the assignment problem (16).
      End-Partial-SA
    (b) Compute  $\mathcal{L}^* = \mathcal{L}_{s^*, \nu^*}^{(t)}$ .
    (c) Set  $(s^{(t,b)}, \nu^{(t,b)}) = (s^*, \nu^*)$  and  $\mathcal{L}^{(t,b)} = \mathcal{L}^*$  with probability
      
$$P((s^{(t,b-1)}, \nu^{(t,b-1)}) \rightarrow (s^*, \nu^*)) = \begin{cases} \exp\left\{-\frac{\mathcal{L}^* - \mathcal{L}^{(t,b-1)}}{T_b}\right\} & \text{if } \mathcal{L}^* - \mathcal{L} > 0 \\ 1 & \text{if } \mathcal{L}^* - \mathcal{L} \leq 0. \end{cases}$$

      otherwise set  $(s^{(t,b)}, \nu^{(t,b)}) = (s^{(t,b-1)}, \nu^{(t,b-1)})$  and  $\mathcal{L}^{(t,b)} = \mathcal{L}^{(t,b-1)}$ .
  endfor
Step 3: Set  $(s^{(t)}, \nu^{(t)}) = (s^{(t,B)}, \nu^{(t,B)})$ .


---


  END of SP-SA Step.

```

The overall procedure for the two simulated annealing schemes is described in Algorithm 3. Clearly, one iteration of the Partial SA scheme is more expensive computationally than one iteration of the Full SA scheme. But since the proposal mechanism in Partial SA minimizes $\mathcal{L}(s, \nu)$ given s , it is expected that it will converge faster to the solution compared to Full SA where both parameters are randomly proposed. This is empirically illustrated in Section B of the Appendix.

For both SA schemes, the cooling schedule $\{T_b, b = 1, 2, \dots\}$ is such that $T_b > 0$ for all b and $\lim_{b \rightarrow \infty} T_b = 0$. Romeo and Sangiovanni-Vincentelli (1991) showed that a logarithmic cooling schedule of the form $T_b = \gamma / \log(b + \gamma_0)$, $b = 1, 2, \dots$, is a sufficient condition for convergence with probability one to the optimal solution. In our applications, a reasonable trade-off between accuracy and computing time was obtained with $\gamma = \gamma_0 = 1$ and a total number of annealing loops $20 \leq B \leq 2000$.

3.4. Toy example: Geometrical illustration for $q = 2$ factors

A geometrical illustration of the proposed method is provided in Figure 1, for the special case of $q = 2$ factors. Figure 1.(a) shows the scatterplot of the ordered pairs $(\lambda_{r1}^{(t)}, \lambda_{r2}^{(t)})$ for variable $r = 1, 2, 3$ (corresponding to distinct symbols), where $t = 1, \dots, 10$ denotes a given MCMC draw. The large variability of the MCMC draws suggest that the output of factor loadings is not identifiable due to rotation, sign and permutation invariance. For illustration purposes, a particular MCMC draw is emphasized, with values equal to

$$\Lambda = \begin{pmatrix} 0.02 & 0.00 \\ -0.63 & 0.55 \\ 0.47 & 0.71 \end{pmatrix},$$

where each row of the matrix above corresponds to the enlarged symbols in Fig 1.(a). Firstly, we apply usual varimax rotations to the whole MCMC output, as shown in Figure 1.(b). The rotated values after this step are displayed in Figure 1.(c). For example, Λ is transformed to

$$\tilde{\Lambda} = \begin{pmatrix} 0.02 & 0.01 \\ -0.84 & 0.06 \\ -0.05 & 0.86 \end{pmatrix}.$$

Note that a simple structure is achieved for each MCMC iteration: each variable loads to at most one factor. However, the factor loadings are still unidentified across the MCMC draws due to sign and permutation invariance.

The final step is to apply Algorithm 1, as shown in Figure 1.(d). In the initialization step of Algorithm 1, the reference matrix of factor loadings is equal to

$$\Lambda^* = \begin{pmatrix} -0.00 & -0.01 \\ -0.20 & 0.15 \\ 0.13 & -0.05 \end{pmatrix}$$

and its rows correspond to the black points shown in Figure 1.(c). The objective function at the initialization step is equal to $\sum_{t=1}^{10} \mathcal{L}_{s^{(t)}, \nu^{(t)}}^{(t)} \approx 13.76$. After 1 iteration

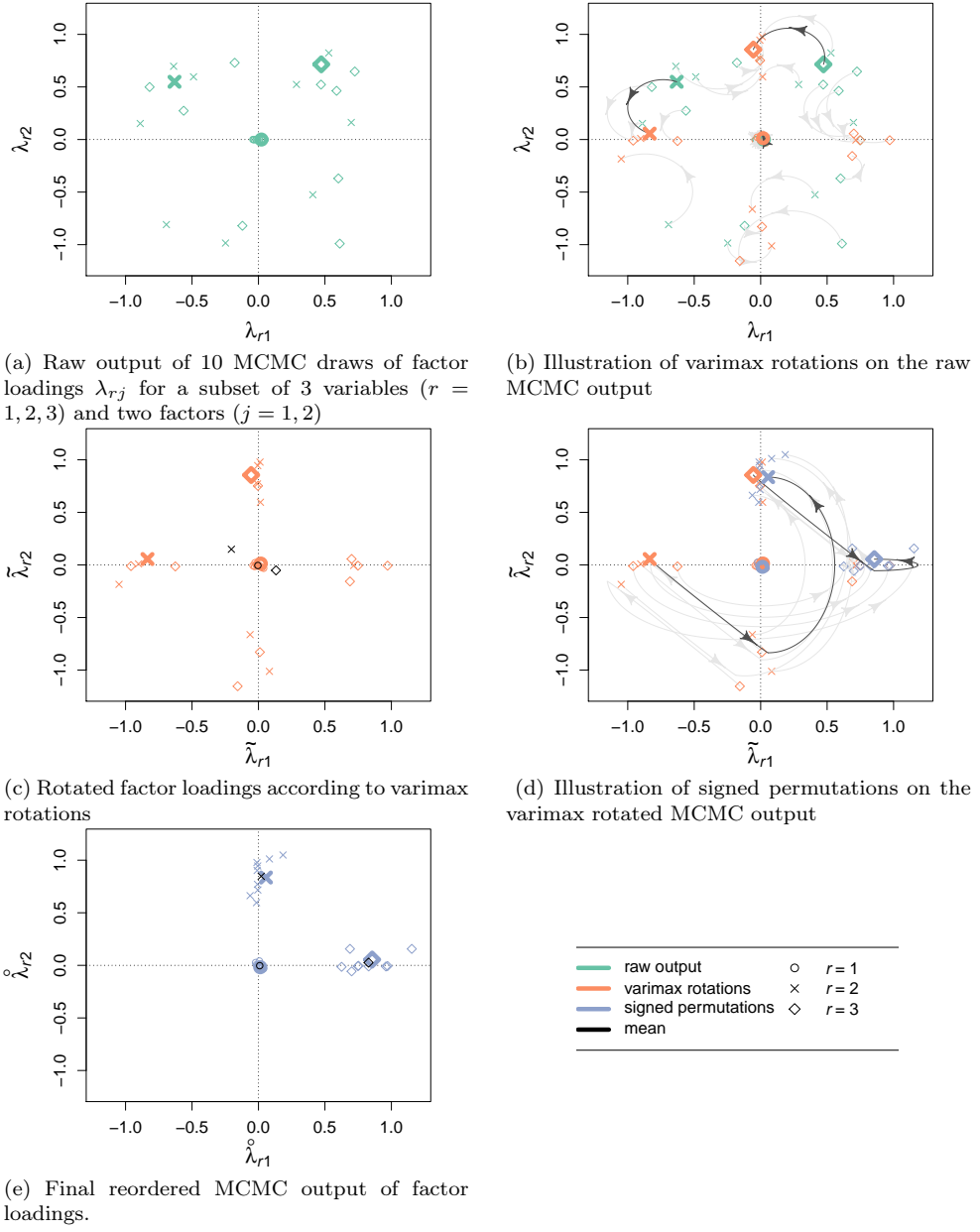


Figure 1: Graphical demonstration of the evolution of the RSP algorithm for $T = 10$ MCMC draws. The highlighted symbols in each panel correspond to a particular MCMC draw. The black symbols in panels (c) and (e) denote the average loadings $(\lambda_{r1}^*, \lambda_{r2}^*)$ per variable across the 10 MCMC draws.

of Steps 1 and 2 of Algorithm 1 the reordered factor loadings correspond to the blue points in Figure 1.(d).

In this case, for each MCMC draw, the transformation consists of a permutation of the index set $\mathcal{T}_2 = \{1, 2\}$ (first segment of the curved arrows) and a sign switching (second segment of the curved arrows). The first transformation means that, for MCMC draw t , $(\tilde{\lambda}_{r1}^{(t)}, \tilde{\lambda}_{r2}^{(t)})$ is transformed to

$$(\dot{\lambda}_{r1}^{(t)}, \dot{\lambda}_{r2}^{(t)}) = (\tilde{\lambda}_{r2}^{(t)}, \tilde{\lambda}_{r1}^{(t)}) \text{ if } \nu^{(t)} = (2, 1)$$

or

$$(\dot{\lambda}_{r1}^{(t)}, \dot{\lambda}_{r2}^{(t)}) = (\tilde{\lambda}_{r1}^{(t)}, \tilde{\lambda}_{r2}^{(t)}) \text{ if } \nu^{(t)} = (1, 2),$$

for $r = 1, 2, 3$. The second part of this step is to apply a sign switch, thus $(\dot{\lambda}_{r1}^{(t)}, \dot{\lambda}_{r2}^{(t)})$ may be transformed to

$$(\mathring{\lambda}_{r1}^{(t)}, \mathring{\lambda}_{r2}^{(t)}) = (-\dot{\lambda}_{r1}^{(t)}, \dot{\lambda}_{r2}^{(t)}) \text{ if } (s_1^{(t)}, s_2^{(t)}) = (-1, 1),$$

or to

$$(\mathring{\lambda}_{r1}^{(t)}, \mathring{\lambda}_{r2}^{(t)}) = (\dot{\lambda}_{r1}^{(t)}, -\dot{\lambda}_{r2}^{(t)}) \text{ if } (s_1^{(t)}, s_2^{(t)}) = (1, -1),$$

or to

$$(\mathring{\lambda}_{r1}^{(t)}, \mathring{\lambda}_{r2}^{(t)}) = (-\dot{\lambda}_{r1}^{(t)}, -\dot{\lambda}_{r2}^{(t)}) \text{ if } (s_1^{(t)}, s_2^{(t)}) = (-1, -1),$$

or even retain the same sign, that is,

$$(\mathring{\lambda}_{r1}^{(t)}, \mathring{\lambda}_{r2}^{(t)}) = (\dot{\lambda}_{r1}^{(t)}, \dot{\lambda}_{r2}^{(t)}) \text{ if } (s_1^{(t)}, s_2^{(t)}) = (1, 1),$$

for $r = 1, 2, 3$. The processed values after this step are displayed in Figure 1.(e) which is the final output returned by our method. Note that the processed output is switched to a simple structure which is coherent across all MCMC iterations.

For example, the values of the emphasized MCMC draw are first permuted according according to $\nu^{(t)} = (2, 1)$ and then switched according to $(s_1^{(t)}, s_2^{(t)}) = (1, -1)$ which corresponds to a reflection with respect to the x axis. The corresponding permutation and reflection matrices are $\mathbf{P} = \begin{pmatrix} 0 & 1 \\ 1 & 0 \end{pmatrix}$ and $\mathbf{S} = \begin{pmatrix} 1 & 0 \\ 0 & -1 \end{pmatrix}$, respectively.

Thus, the signed permutation matrix in this case is $\mathbf{Q} = \mathbf{SP} = \begin{pmatrix} 0 & 1 \\ 1 & 0 \end{pmatrix} \begin{pmatrix} 1 & 0 \\ 0 & -1 \end{pmatrix} = \begin{pmatrix} 0 & -1 \\ 1 & 0 \end{pmatrix}$, implying that $\tilde{\Lambda}$ is finally transformed to

$$\hat{\Lambda} = \tilde{\Lambda}\mathbf{Q} = \tilde{\Lambda}\mathbf{SP} = \begin{pmatrix} 0.02 & 0.01 \\ -0.84 & 0.06 \\ -0.05 & 0.86 \end{pmatrix} \begin{pmatrix} 0 & 1 \\ 1 & 0 \end{pmatrix} \begin{pmatrix} 1 & 0 \\ 0 & -1 \end{pmatrix} = \begin{pmatrix} 0.01 & -0.02 \\ 0.06 & 0.84 \\ 0.86 & 0.05 \end{pmatrix}.$$

The reference matrix of factor loadings is now equal to

$$\Lambda^* = \begin{pmatrix} 0.01 & -0.00 \\ 0.02 & 0.85 \\ 0.83 & 0.03 \end{pmatrix}$$

and the objective function is $\sum_{t=1}^{10} \mathcal{L}_{s^{(t)}, \nu^{(t)}}^{(t)} \approx 0.55$. Subsequent iterations do not improve further this value and Algorithm 1 terminates.

4. Applications

Section 4.1 presents a simulation study and Section 4.2 analyses a real dataset. Section 4.3 deals with mixtures of factor analyzers, using the `fabMix` package (Papastamoulis, 2019, 2018, 2020). In all cases the input data is standardized so the sample means and variances of each variable are equal to 0 and 1 respectively. When the difference between two subsequent evaluations of the objective function in Equation 11 is less than $10^{-6}Tpq$ the algorithm terminates, with T denoting the size of the retained MCMC sample.

In Sections 4.1 and 4.2, the `MCMCpack` package (Martin et al., 2011, 2019) in R was used in order to fit Bayesian FA models. The default normal priors are placed upon the factor loadings and factor scores while inverse Gamma priors are assumed for the uniquenesses, that is,

$$\begin{aligned}\lambda_{rj} &\sim \mathcal{N}(l_0, L_0^{-1}), \\ \sigma_r^2 &\sim \mathcal{IG}(a_0/2, b_0/2)\end{aligned}$$

mutually independent for $r = 1, \dots, p$; $j = 1, \dots, q$. We used the default prior parameters of the package, that is, $l_0 = 0$, $L_0 = 0$, $a_0 = b_0 = 0.001$. Note that the specific choices correspond to an improper prior distribution on the factor loadings and a vaguely informative prior distribution on the uniquenesses. In addition, all factor loadings were assumed unconstrained, that is, the “`lambda.constraints`” option was disabled.

The implementation is performed via the `MCMCfactanal()` function, which applies standard Gibbs sampling (Gelfand and Smith, 1990) in order to generate MCMC samples from the posterior distribution. In all cases, a MCMC sample of two million iterations was simulated, following a burn-in period of $10K$ iterations; where K here denotes one thousand. Finally, a thinned MCMC sample of $10K$ draws was retained for inference, keeping the simulated values of every 200th MCMC iteration. Highest Posterior Density (HPD) are computed by the `HDIinterval` package (Meredith and Kruschke, 2018). Simultaneous credible regions are computed as described in Besag et al. (1995), using the implementation in the R package `bayesSurv` (García-Zattera et al., 2016). In Section 4.1 we have also used the `BayesFM` package (Piatek, 2019) in order to compare our findings with the ones arising from the method of Conti et al. (2014).

4.1. Simulation study

At first we illustrate the proposed approach using two simulated datasets: in dataset 1 there are $n = 100$ observations, $p = 8$ variables and $q_{\text{true}} = 2$ factors, while in dataset 2 we set $n = 200$, $p = 24$ and $q_{\text{true}} = 4$. The association patterns between the generated variables and the assumed underlying factors is summarized in Table 1.

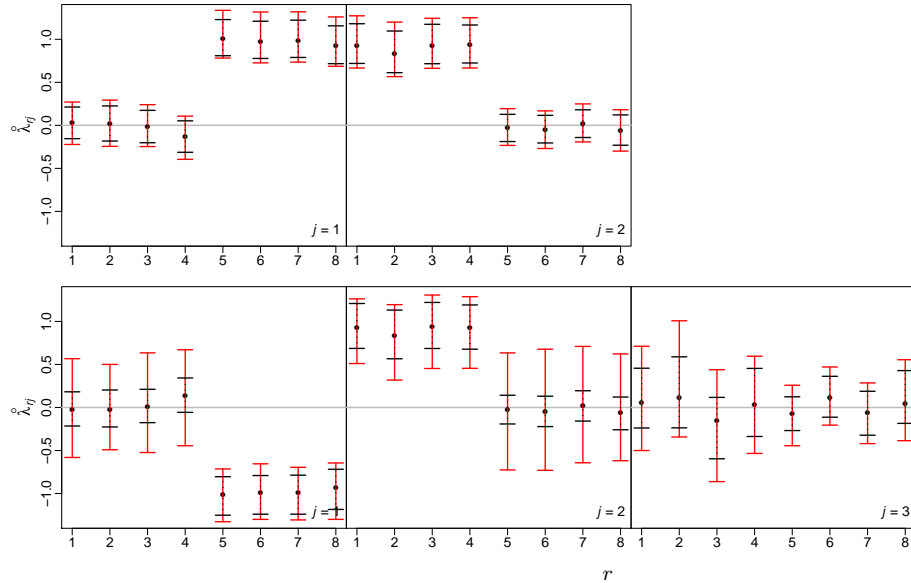


Figure 2: *Simulated data 1*: 99% HPD intervals (black) and simultaneous 99% credible regions (red) of reordered factor loadings, when fitting Bayesian FA models with $q = 2$ (top) and $q = 3$ (bottom) factors (Dataset details: $p = 8$ variables and $q_{\text{true}} = 2$ factors).

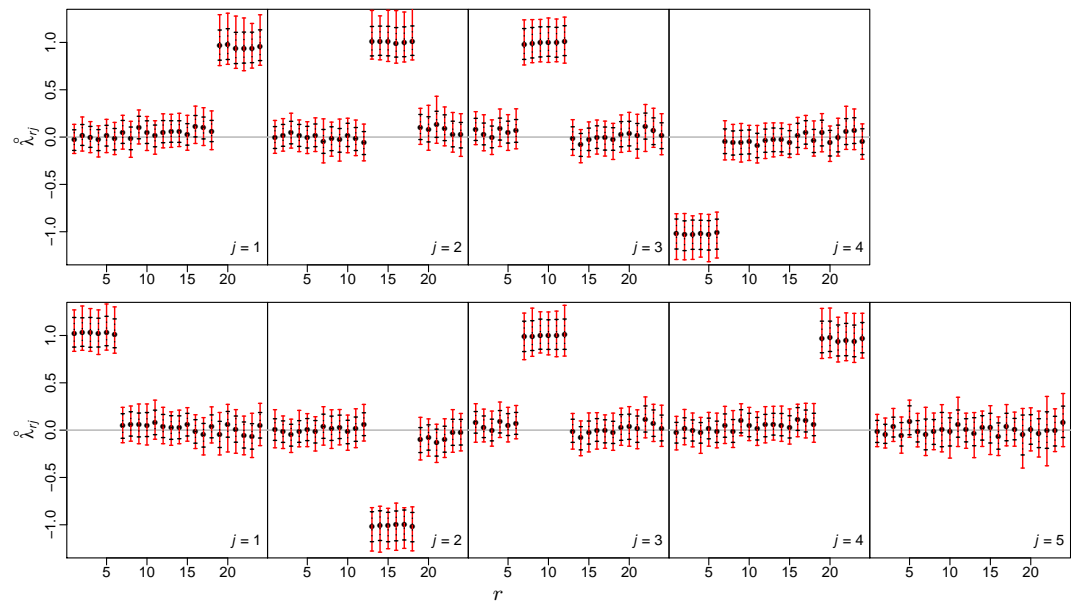


Figure 3: *Simulated data 2*: 99% HPD intervals (black) and simultaneous 99% credible regions (red) of reordered factor loadings, when fitting Bayesian FA models with $q = 4$ (top) and $q = 5$ (bottom) factors (Dataset details: $n = 200$, $p = 24$ and $q_{\text{true}} = 4$).

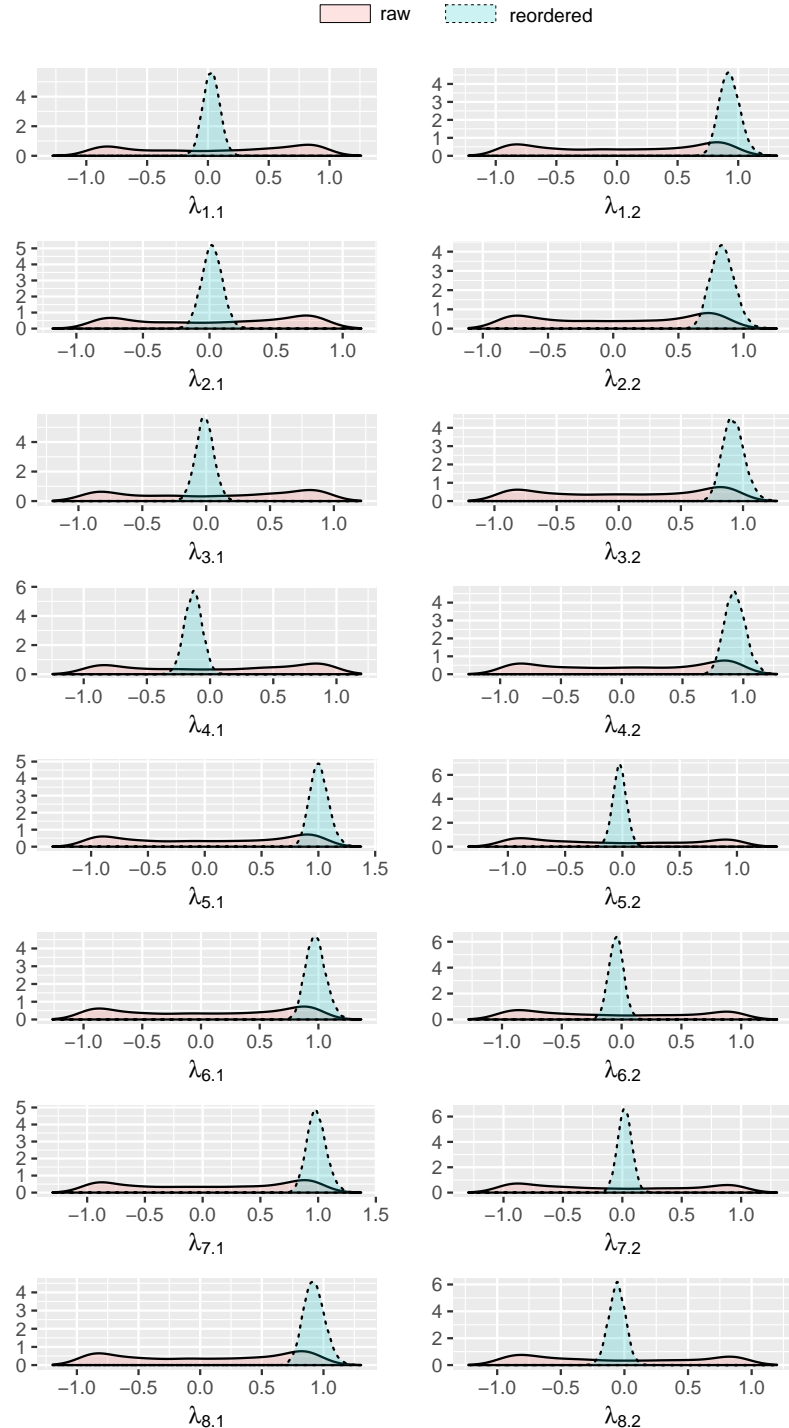


Figure 4: *Simulated data 1*: Marginal posterior distribution of raw and reordered factor loadings, conditional on the true number of factors ($q = q_{\text{true}} = 2$).

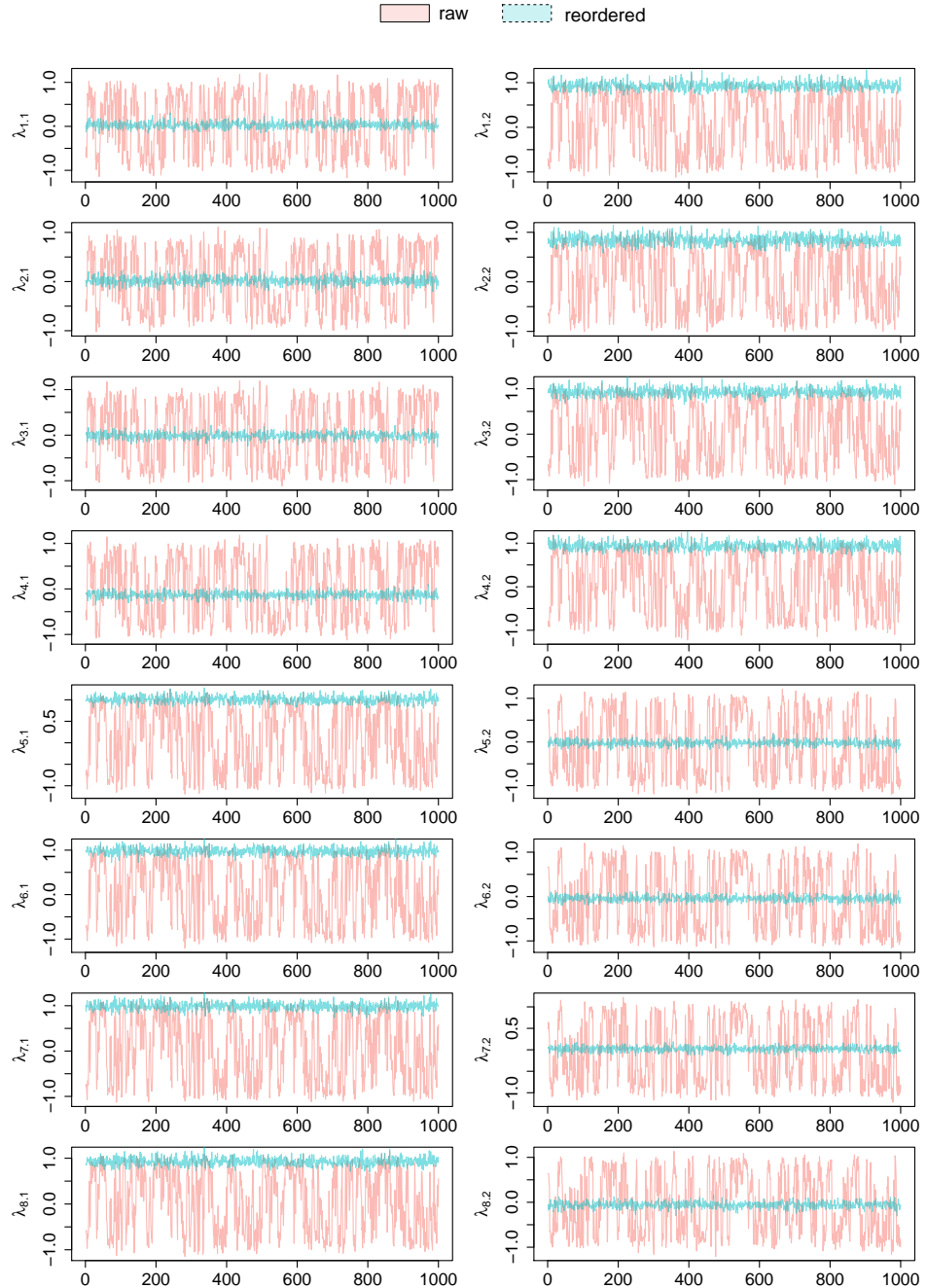


Figure 5: *Simulated data 1*: MCMC trace of raw and reordered factor loadings, conditional on the true number of factors (Thinned sample of 1000 iterations; $q = q_{\text{true}} = 2$).

For more details on the simulation procedure, the reader is referred to [Papastamoulis \(2018, 2020\)](#).

	n	p	Factors			
			F_1	F_2	F_3	F_4
Example 1	100	8	$Y_1 - Y_4$	$Y_5 - Y_8$		
Example 2	200	24	$Y_1 - Y_6$	$Y_7 - Y_{12}$	$Y_{13} - Y_{18}$	$Y_{19} - Y_{24}$

TABLE 1
Simulation study plan of Section 4.1

Figures 2 and 3 display the 99% highest posterior density intervals and a 99% simultaneous credible region of reordered factor loadings, when fitting Bayesian FA models with $q_{\text{true}} \leq q \leq q_{\text{true}} + 1$. In particular, each panel contains the intervals for each column of the $p \times q$ matrix $\hat{\Lambda}$. Observe that for $q > q_{\text{true}}$ there are $q - q_{\text{true}}$ columns of $\hat{\Lambda}$ with all intervals including zero. For dataset 1, a detailed view of the marginal posterior distributions of raw and reordered factor loadings when the number of factors is equal to its true value ($q = 2$) is shown in Figure 4. The corresponding (thinned) MCMC trace is shown in Figure 5. Note the broad range of the posterior distributions of the raw factor loadings (shown in red), which is a consequence of non-identifiability. On the other hand, the bulk of the posterior distributions of the reordered factor loadings is concentrated close to 0 or ± 1 . See also Figure A.1 in Appendix A for a comparison of multiple MCMC chains.

The inspection of the simultaneous credible regions reveals possible overfitting of the model being used in each case. This is indeed the case with the 3-factor model at Example 1 and the 5-factor model at Example 2. Clearly, the simultaneous credible regions at Figures 3 and 2 are able to detect that there is one redundant column at the matrix of factor loadings. Although this is not a proper Bayesian model selection scheme, we observed that this procedure can successfully detect cases of overfitting, provided that the number of factors is indeed larger than the “true” one.

In order to further assess the ability of this approach in order to detect over-fitted factor models, we have simulated synthetic datasets from (1) with $p = 16$ or $p = 24$ variables. The true number of factors was set equal to $q_{\text{true}} = 2$ or $q_{\text{true}} = 4$ (for $p = 16$) and $q_{\text{true}} = 6$ (for $p = 24$). For each simulated dataset, the sample size (n) is chosen at random from the set $\{100, 200\}$, the idiosyncratic variances are randomly drawn from the set $\sigma_r^2 = \sigma^2$, $r = 1, \dots, p$ with σ^2 randomly drawn from the set $\{400, 800, 1200\}$.

Let q_0 denotes the number of redundant columns of $\hat{\Lambda}$ for a FA model with q factors, that is, the number of columns of $\hat{\Lambda}$ where at least one interval in the $(p \times q)$ -dimensional 99% Simultaneous Credible Region (SCR) is not containing 0. Now define the number of “effective” columns of $\hat{\Lambda}$ as $\hat{q} = q - q_0$. In order to give an empirical comparison of \hat{q} with model selection approaches for estimating the number of factors, we compare our findings with the Bayesian Information Criterion using the same output from the MCMCpack package, as well as with the stochastic search method of [Conti et al. \(2014\)](#) as implemented in the R package `BayesFM` ([Piatek, 2019](#)).

We generated MCMC samples for a total number of $T = 100K$ iterations following a burn-in period of $10K$, using the default prior assumptions in both packages. The number of factors varied in the set $1 \leq q \leq q_{\text{true}} + 2$. Note however that the minimum

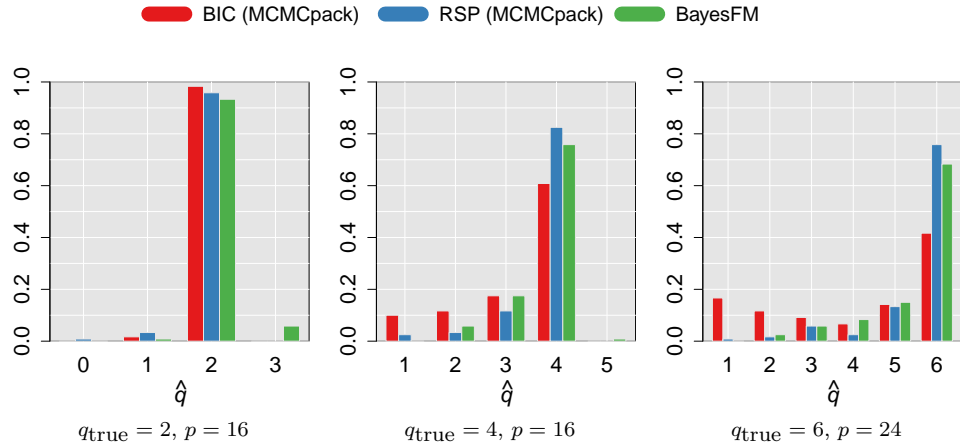


Figure 6: Comparison of the “effective” number of columns of $\hat{\Lambda}$ (“MCMCpack RSP”) with model selection procedures (“MCMCpack BIC” and “BayesFM”), when fitting FA models. The barplots display relative frequencies of \hat{q} corresponding to the maximum number of factors per method.

acceptable number of factors in BayesFM is 2. According to [Conti et al. \(2014\)](#), the maximum number of factors in order to ensure identifiability of their model cannot exceed $\min\{p/3, \phi(p)\}$, implying that in the $p = 16$ scenario the maximum number of factors for BayesFM is 5.

For each combination of p and q_{true} , 120 datasets were simulated and the results are summarized in Figure 6. We observe that the number of “effective” columns of $\hat{\Lambda}$ is fairly consistent with the active number of factors inferred by BayesFM. As the true number of factors grows larger, BIC favours more parsimonious models. Overall, we conclude that our reordering approach can successfully identify over-fitted models as long as $q > q_{\text{true}}$. More challenging simulation studies with up to $q = 50$ factors are presented in Appendix B.

4.2. The Grant-White school dataset

In this example we use scores on nine mental ability test scores of seventh and eighth grade children from two different schools (Pasteur and Grant-White) in Chicago. The data were first published in [Holzinger and Swineford \(1939\)](#) and they are publicly available through the `lavaan` package ([Rosseel, 2012](#)) in R. This is a well-known data set used in the LISREL ([Joreskog et al., 1999](#)), AMOS ([Arbuckle et al., 2010](#)) and Mplus ([Muthén and Muthén, 2019](#)) tutorials to illustrate a three-factor model for normal data. Variables 1-3 (visual perception, cubes and lozenges) denote “visual perception”, variables 4-6 (paragraph comprehension, sentence completion and word meaning) are related to verbal “verbal ability”, and variables 7-9 (speeded addition, speeded counting of dots, speeded discrimination straight and curved capitals) are

connected to “speed”. Following Jöreskog (1969); Mavridis and Ntzoufras (2014), we used the subset of 145 students from the Grant-White school.

		$q = 3$			$q = 4$			
		1	2	3	1	2	3	4
visual	Y_1	−0.28	0.19	0.64*	0.47	0.41	0.12	0.26
	Y_2	−0.16	0.08	0.49*	0.14	0.52*	0.07	0.15
	Y_3	−0.28	0.11	0.63*	0.21	0.67*	0.08	0.26
verbal	Y_4	−0.89*	0.07	0.16	0.11	0.15	0.07	0.89*
	Y_5	−0.84*	0.18	0.11	0.15	0.07	0.16	0.84*
	Y_6	−0.84*	0.07	0.16	0.08	0.16	0.07	0.83*
speed	Y_7	−0.18	0.78*	−0.07	0.05	−0.04	0.83*	0.17
	Y_8	−0.03	0.83*	0.24	0.24	0.16	0.77*	0.03
	Y_9	−0.26	0.54*	0.45*	0.48	0.26	0.45*	0.24

TABLE 2
Grant-White school dataset: RSP Estimated posterior means of factor loadings for the 3 and 4 factor models.

Notes: Yellow boxes and asterisks: loadings with simultaneous 99% credible region that does not contain zero.

First column of 4-Factor model ($q = 4$): is redundant since for all loadings the zero value is a reasonable posterior value.

We fitted factor models consisting of $q = 3$ and $q = 4$ factors. The corresponding posterior mean estimates of reordered factor loadings is displayed in Table 2. When using a model with $q = 3$ factors we conclude that Factor 1 is mostly associated with variables 4-6, that is, the “verbal ability” group. Factor 2 is associated with variables 7-9, that is, the “speed” group. Factor 3 is mostly associated with variables 1-3, that is, the “visual perception” group. Notice however that variable 9 is also loading on the 3rd factor. These points are coherent with the analysis of Mavridis and Ntzoufras (2014). When using a model with $q = 4$ factors, the simultaneous 99% credible region contains zero for all loadings of the first column of $\hat{\Lambda}$, so there is evidence that there is one redundant factor. The raw and reordered outputs for the model with $q = 3$ factors is shown in Figure 7.

4.3. Mixtures of Factor Analyzers

Mixtures of Factor Analyzers (Ghahramani et al., 1996; McLachlan et al., 2003; Fokoué and Titterington, 2003; McLachlan et al., 2011; McNicholas and Murphy, 2008; McNicholas, 2016; Malsiner Walli et al., 2016, 2017; Frühwirth-Schnatter and Malsiner-Walli, 2019; Murphy et al., 2018; Papastamoulis, 2018, 2020) are generalizations of the typical FA model, by assuming that Equation (6) becomes

$$\mathbf{x}_i \sim \sum_{k=1}^K w_k \mathcal{N}_p \left(\boldsymbol{\mu}_k, \boldsymbol{\Lambda}_k \boldsymbol{\Lambda}_k^\top + \boldsymbol{\Sigma}_k \right), \text{ iid } i = 1, \dots, n \quad (17)$$

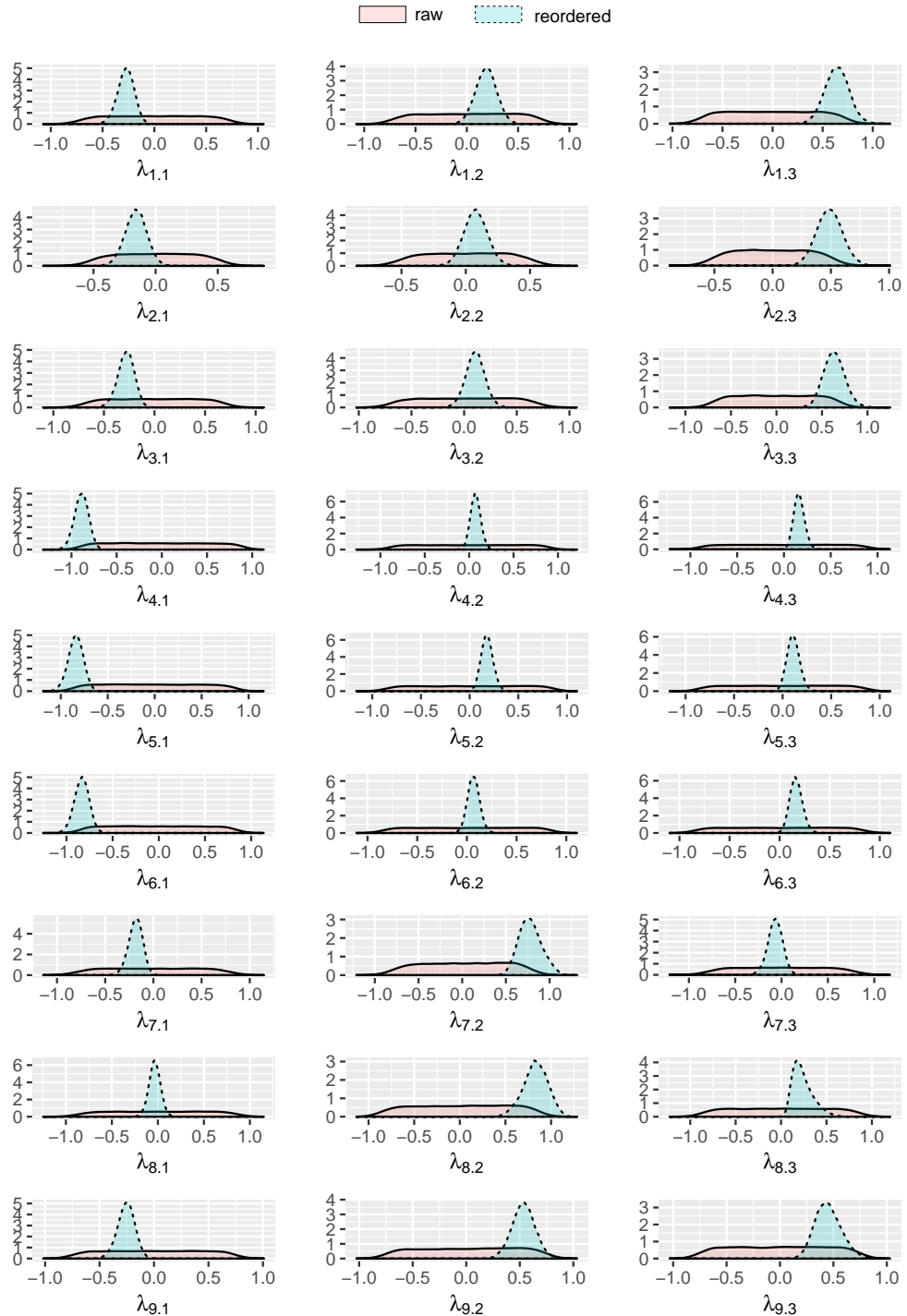


Figure 7: *Grant-White school dataset*: Marginal posterior distribution of raw and reordered factor loadings, using a $q = 3$ factor model.

where K denotes the number of mixture components. The vector of mixing proportions $\mathbf{w} := (w_1, \dots, w_K)$ contains the weight of each component, with $0 \leq w_k \leq 1$; $k = 1, \dots, K$ and $\sum_{k=1}^K w_k = 1$. Note that the mixture components are characterized by different parameters $\boldsymbol{\mu}_k, \boldsymbol{\Lambda}_k, \boldsymbol{\Sigma}_k$, $k = 1, \dots, K$. Thus, MFAs are particularly useful when the observed data exhibits unusual characteristics such as heterogeneity. The reader is referred to [Papastamoulis \(2020\)](#) for details of the prior distributions. A difference is that now the factor loadings are assumed unconstrained, in contrast to the original modelling approach of [Papastamoulis \(2020\)](#) where the lower triangular expansion in Equation (7) was enabled.

		Variables									
		Y_1	Y_2	Y_3	Y_4	Y_5	Y_6	Y_7	Y_8	Y_9	Y_{10}
Cluster 1	Factor 1	1.0	1.0	1.0	1.0	1.0	0.0	0.0	-0.0	-0.0	-0.0
	Factor 2	0.0	-0.0	0.0	0.0	-0.0	-1.0	-1.0	-1.0	-1.0	-1.0
Cluster 2	Factor 1	0.0	-0.0	-0.0	-0.0	-0.0	0.5	0.5	0.5	0.5	0.5
	Factor 2	-0.0	0.0	-0.0	0.0	-0.0	0.0	-0.0	-0.0	0.0	-0.0

TABLE 3
True factor loadings values for the simulated dataset with 2 clusters (up to a multiplicative constant).

We considered a simulated dataset of $n = 100$ and $p = 10$ -dimensional observations with $K = 2$ clusters. The real values of factor loadings per cluster are shown in Table 3. The correlation matrix per cluster is shown in Figure 8. Notice that the 1st cluster consists of 2 factors, while cluster 2 consists of 1 active factor since the second column is redundant. This is a rather challenging scenario because the posterior distribution suffers from many sources of identifiability problems: At first, all component-specific parameters (including the factor loadings per cluster) are not identifiable due to the label switching problem of Bayesian mixture models. Next, the factor loadings within each cluster are not identifiable due to rotation, sign and permutation invariance.

The `fabMix` package ([Papastamoulis, 2019, 2018, 2020](#)) was used in order to produce a MCMC sample from the posterior distribution of the MFA model, using a prior parallel tempering scheme with 4 chains and a number of MCMC iterations equal to 100K, following a burn-in period of 10K iterations. A thinned MCMC sample of 10K iterations was retained for inference. We considered an overfitted mixture model with $K_{\max} = 5$ number of components under the constraint $\boldsymbol{\Sigma}_1 = \dots = \boldsymbol{\Sigma}_K$ (that is, the “UCU” parameterization in the `fabMix` nomenclature) in (17). Two different factor levels were fitted, that is, models with $q = 2$ and $q = 3$ factors. In both cases, the most-probable number of clusters is 2, that is, the true value. Using the Bayesian Information Criterion ([Schwarz, 1978](#)) for choosing q , the selected model corresponds to $q = 2$ factors, however we present the results for both values of factor levels. The raw output of the MCMC sampler is first post-processed according to the Equivalence Classes Representatives (ECR) algorithm ([Papastamoulis and Iliopoulos, 2010](#)) in order to deal with the label switching between mixture components. Next, the proposed method was applied within each cluster in order to correct the rotation-sign-permutation invariance of factors. The resulting simultaneous 99% credible region of the reordered output of factor loadings is displayed in Figure 9.

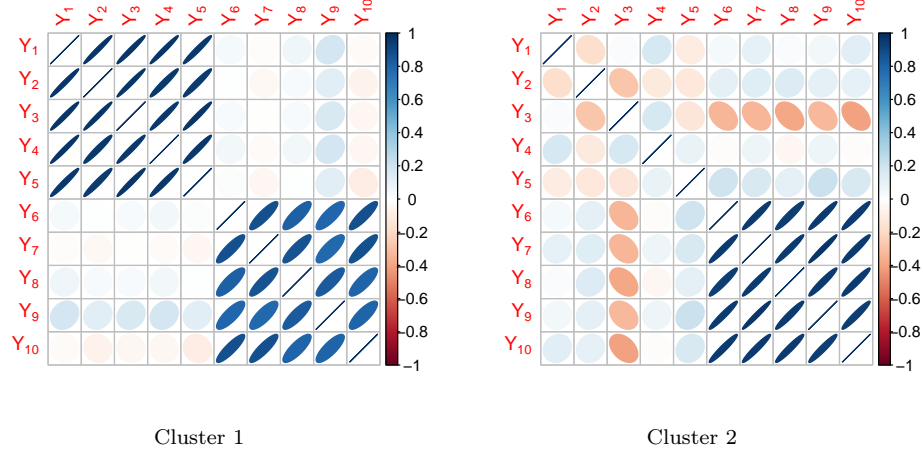


Figure 8: Correlation matrix per cluster for the simulated dataset.

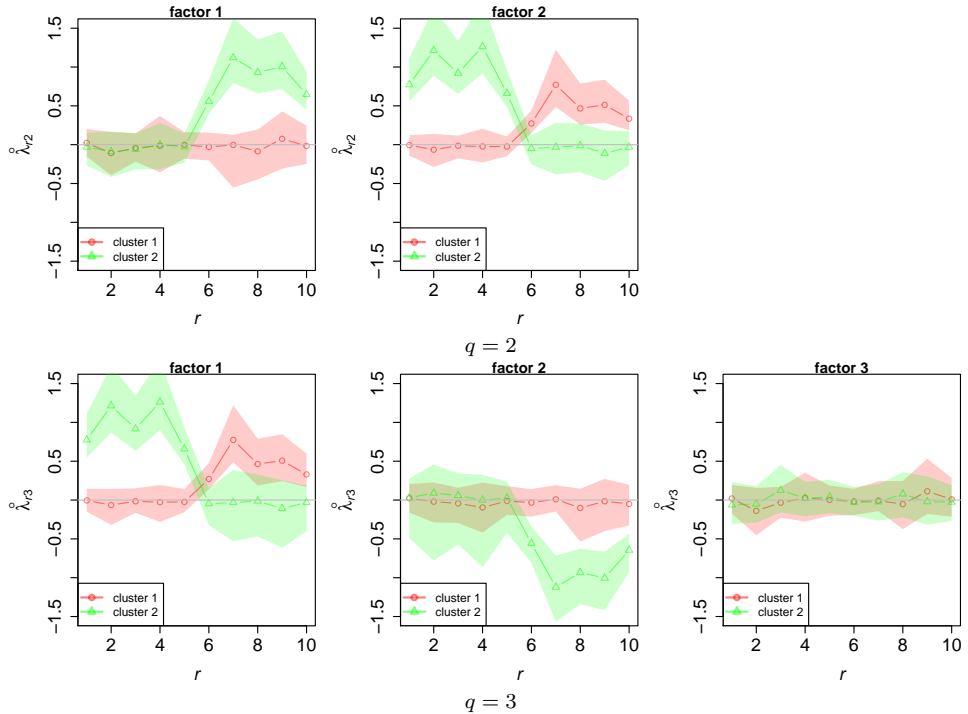


Figure 9: Post-processed factor loadings per cluster for the simulated dataset with $K = 2$ clusters, when fitting Bayesian Mixtures of Factor Analyzers with q factors.

More specifically, when the number of factors is set equal to 2, there is one cluster (coloured red) where the simultaneous credible region of all loadings of the factor labelled as “factor 1” contains zero, while the loadings of the factor labelled as “factor 2” are different than zero for all variables $r \geq 6$. This is the correct structure of loadings for cluster 2 in Table 3. In addition, there is another cluster (coloured green) where the simultaneous credible region of all loadings of the factor labelled as “factor 1” does not contain zero for all $r \geq 6$, while the loadings of the factor labelled as “factor 2” are different than zero for all variables $r \leq 5$. When the number of factors in the MCMC sampler is set equal to $q = 3$ (larger than its true value by one), observe that the simultaneous credible region of the factor labelled as “factor 3” Figure 9 contains zero. We conclude that, up to a switching of cluster labels and a signed permutation of factors within each cluster, the proposed approach successfully identifies the structure of true factor loadings. A second illustration of the proposed methodology using mixtures of factor analyzers to a publicly available dataset is presented in Appendix C.

5. Discussion

The problem of posterior identification of Bayesian Factor Analytic models has been addressed using a post-processing approach. Up to our knowledge, this is the first work where posterior identification of Bayesian Factor models is achieved without extending the hierarchical structure of the typical FA model, as summarized in Equations 1–5. According to our simulation studies and the implementation to real life datasets, the proposed method leads to meaningful posterior summaries. We also demonstrated that the reordered MCMC sample can successfully identify cases of over-fitted models, where in such cases the credible region of factor loadings contains zeros for the corresponding redundant columns of Λ . Our method is also relevant to the model-based clustering community as shown in the applications on mixtures of factor analyzers (Section 4.3 and Appendix C). Comparison of multiple chains is also possible after coupling the pipeline with one extra reordering step as discussed in Appendix A.

The proposed method first proceeds by applying usual varimax rotations on the generated MCMC sample. We have also used oblique rotations (Hendrickson and White, 1964) and we obtained essentially the same answers. Then, we minimize the loss function in Equation 11, which is carried out in an iterative fashion as shown in Algorithm 1: given the sign (s) and permutation (ν) variables, the matrix Λ^* is set equal to the mean of the reordered factor loadings. Given Λ^* , s and ν are chosen in order to minimize the expression in Equation 15. In order to minimize (15), we solve one assignment problem (see Equation 16) for each value of s (per MCMC iteration), as detailed in Section 3.3. This approach works within reasonable computing time for typical values of the number of factors (e.g. $q \leq 10$).

For larger values of q , we propose two approximate solutions based on simulated annealing. Simulation based details concerning the computing time for each proposed scheme for models with different numbers of factors (up to $q = 50$) are provided in Appendix B. In these cases we have generated MCMC samples using Hamiltonian Monte Carlo techniques implemented in the Stan (Carpenter et al., 2017; Stan Development Team, 2019) programming language. According to these empirical findings,

the two simulated annealing based algorithms are very effective, rapidly decreasing the objective function within reasonable computing time. Nevertheless, the partial simulated annealing algorithm should be preferred since it reaches solutions close to the true minimum faster than the full annealing scheme. This finding was expected since the proposal mechanism in Partial SA is more elaborate compared to the completely random proposal in Full SA.

Finally, the authors are considering the implementation of the proposed approach in combination with Bayesian variable selection methods such as stochastic search variable selection – SSVS (George and McCulloch, 1993; Mavridis and Ntzoufras, 2014), Gibbs variable selection – GVS (Dellaportas et al., 2002) and/or reversible jump MCMC – RJMCMC (Green, 1995). The implementation of the method might solve not only identifiability problems but also provide more robust results for Bayesian variable selection methods where the specification of the prior distribution is crucial due the Lindley–Bartlett paradox. Moreover, in this paper, our proposed method is used as a post-processing tool for the estimation of the posterior distribution of factor loadings within each model. For Bayesian variable selection, the implementation of the Varimax-RSP algorithm within each MCMC might be influential for the selection of items and factor structure. For this reason, a thorough study (theoretical and empirical) and comparison between the post-processing and the within-MCMC implementation of the method is needed.

Supplementary Material

Appendix: Appendix

(https://github.com/mqbsspppe/factor_switching). Contents: *Appendix A*: Comparison of multiple chains. *Appendix B*: Computational benchmark: Performance comparison in high dimensional factor analytic models. *Appendix C*: Illustration of mixtures of factor analyzers in publicly available data: The Wave dataset.

Supplement B: Source code

(<http://CRAN.R-project.org/package=factor.switching>). R package `factor.switching` available at the Comprehensive R Archive Network (R Core Team, 2018).

Supplement C: Reproducibility

(https://github.com/mqbsspppe/factor_switching). This repository contains scripts that reproduce the results for both simulated and real data.

References

Aguilar, O. and West, M. (2000). “Bayesian Dynamic Factor Models and Portfolio Allocation.” *Journal of Business & Economic Statistics*, 18(3): 338–357.
URL <http://www.jstor.org/stable/1392266>

Anderson, T. W. and Rubin, H. (1956). “Statistical inference in factor analysis.” In *Proceedings of the third Berkeley symposium on mathematical statistics and probability*, volume 5, 111–150.

Arbuckle, J. L. et al. (2010). "IBM SPSS Amos 19 user's guide." *Crawfordville, FL: Amos Development Corporation*, 635.

Arminger, G. and Muthén, B. O. (1998). "A Bayesian approach to nonlinear latent variable models using the Gibbs sampler and the Metropolis-Hastings algorithm." *Psychometrika*, 63(3): 271–300.

Bartholomew, D. J., Knott, M., and Moustaki, I. (2011). *Latent variable models and factor analysis: A unified approach*, volume 904. John Wiley & Sons.

Bekker, P. A. and ten Berge, J. M. (1997). "Generic global identification in factor analysis." *Linear Algebra and its Applications*, 264: 255 – 263.

Berkelaar, M. et al. (2013). *lpSolve: Interface to Lp_solve v. 5.5 to solve linear/integer programs*. R package version 5.6.13.3.
URL <http://CRAN.R-project.org/package=lpSolve>

Besag, J., Green, P., Higdon, D., Mengerson, K., et al. (1995). "Bayesian computation and stochastic systems." *Statistical science*, 10(1): 3–41.

Bhattacharya, A. and Dunson, D. B. (2011). "Sparse Bayesian infinite factor models." *Biometrika*, 291–306.

Breiman, L., Friedman, J., Olshen, R., and Stone, C. (1984). *Classification and regression trees*. Wadsworth International Group: Belmont, California.

Brooks, S. P. and Gelman, A. (1998). "General methods for monitoring convergence of iterative simulations." *Journal of computational and graphical statistics*, 7(4): 434–455.

Burkard, R., Dell'Amico, M., and Martello, S. (2009). *Assignment Problems*. SIAM e-books. Society for Industrial and Applied Mathematics (SIAM, 3600 Market Street, Floor 6, Philadelphia, PA 19104).
URL <http://books.google.co.uk/books?id=nH1zbApL0r0C>

Carpenter, B., Gelman, A., Hoffman, M., Lee, D., Goodrich, B., Betancourt, M., Brubaker, M., Guo, J., Li, P., and Riddell, A. (2017). "Stan: A Probabilistic Programming Language." *Journal of Statistical Software, Articles*, 76(1): 1–32.
URL <https://www.jstatsoft.org/v076/i01>

Carvalho, C. M., Chang, J., Lucas, J. E., Nevins, J. R., Wang, Q., and West, M. (2008). "High-dimensional sparse factor modeling: applications in gene expression genomics." *Journal of the American Statistical Association*, 103(484): 1438–1456.

Conti, G., Frühwirth-Schnatter, S., Heckman, J. J., and Piatek, R. (2014). "Bayesian exploratory factor analysis." *Journal of Econometrics*, 183(1): 31 – 57. Internally Consistent Modeling, Aggregation, Inference and Policy.
URL <http://www.sciencedirect.com/science/article/pii/S0304407614001493>

Dellaportas, P., Forster, J., and Ntzoufras, I. (2002). "On Bayesian Model and Variable Selection Using MCMC." *Statistics and Computing*, 12: 27–36.

Fokoué, E. and Titterington, D. (2003). "Mixtures of factor analysers. Bayesian estimation and inference by stochastic simulation." *Machine Learning*, 50(1-2): 73–94.

Frühwirth-Schnatter, S. and Malsiner-Walli, G. (2019). "From here to infinity: Sparse finite versus Dirichlet process mixtures in model-based clustering." *Advances in Data Analysis and Classification*, 13: 33–64.

García-Zattera, M. J., Jara, A., and Komárek, A. (2016). "A flexible AFT model for misclassified clustered interval-censored data." *Biometrics*, 72(2): 473–483.

Gelfand, A. and Smith, A. (1990). "Sampling-based approaches to calculating marginal densities." *Journal of American Statistical Association*, 85: 398–409.

Gelman, A., Rubin, D. B., et al. (1992). "Inference from iterative simulation using multiple sequences." *Statistical science*, 7(4): 457–472.

George, E. and McCulloch, R. (1993). "Variable Selection via Gibbs Sampling." *Journal of the American Statistical Association*, 88: 881–889.

Geweke, J. and Zhou, G. (1996). "Measuring the pricing error of the arbitrage pricing theory." *The review of financial studies*, 9(2): 557–587.

Ghahramani, Z., Hinton, G. E., et al. (1996). "The EM algorithm for mixtures of factor analyzers." Technical report, Technical Report CRG-TR-96-1, University of Toronto.

Green, P. (1995). "Reversible Jump Markov chain Monte Carlo Computation and Bayesian Model Determination." *Biometrika*, 82: 711–732.

Hendrickson, A. E. and White, P. O. (1964). "Promax: A quick method for rotation to oblique simple structure." *British journal of statistical psychology*, 17(1): 65–70.

Holzinger, K. J. and Swineford, F. (1939). "A study in factor analysis: The stability of a bi-factor solution." *Supplementary Educational Monographs*.

Jöreskog, K. G. (1969). "A general approach to confirmatory maximum likelihood factor analysis." *Psychometrika*, 34(2): 183–202.

Jöreskog, K. G., Sorbom, D., Du Toit, S., and Du Toit, M. (1999). "LISREL 8: New statistical features." *Chicago: Scientific Software International*, 6–7.

Kaiser, H. F. (1958). "The varimax criterion for analytic rotation in factor analysis." *Psychometrika*, 23(3): 187–200.

Kim, J.-O. and Mueller, C. W. (1978). *Factor analysis: Statistical methods and practical issues*, volume 14. Sage.

Kirkpatrick, S., Gelatt, C. D., and Vecchi, M. P. (1983). "Optimization by simulated annealing." *SCIENCE*, 220(4598): 671–680.

Lawley, D. and Maxwell, A. (1962). "Factor analysis as a statistical method." *Journal of the Royal Statistical Society. Series D (The Statistician)*, 12(3): 209–229.

Ledermann, W. (1937). "On the rank of the reduced correlational matrix in multiple-factor analysis." *Psychometrika*, 2(2): 85–93.

Lopes, H. F. and West, M. (2004). "Bayesian model assessment in factor analysis." *Statistica Sinica*, 14(1): 41–68.

Lucas, J., Carvalho, C., Wang, Q., Bild, A., Nevins, J. R., and West, M. (2006). "Sparse statistical modelling in gene expression genomics." *Bayesian inference for gene expression and proteomics*, 1: 0–1.

Malsiner Walli, G., Frühwirth-Schnatter, S., and Grün, B. (2016). "Model-based clustering based on sparse finite Gaussian mixtures." *Statistics and Computing*, 26: 303–324.

— (2017). "Identifying Mixtures of Mixtures Using Bayesian Estimation." *Journal of Computational and Graphical Statistics*, 26: 285–295.

Martin, A. D., Quinn, K. M., and Park, J. H. (2011). "MCMCpack: Markov Chain Monte Carlo in R." *Journal of Statistical Software*, 42(9): 22.

URL <http://www.jstatsoft.org/v42/i09/>

Martin, A. D., Quinn, K. M., Park, J. H., Vieilledent, G., Maleck, M., Blackwell, M., Poole, K., Reed, C., Goodrich, B., Ihaka, R., "The R Development Core Team",

"The R Foundation", L'Ecuyer, P., Matsumoto, M., and Nishimura, T. (2019). *MCMCpack: Markov Chain Monte Carlo (MCMC) Package*. R package version 1.4-5.

URL <http://CRAN.R-project.org/package=MCMCpack>

Mavridis, D. and Ntzoufras, I. (2014). "Stochastic search item selection for factor analytic models." *British Journal of Mathematical and Statistical Psychology*, 67(2): 284–303.

URL <https://onlinelibrary.wiley.com/doi/abs/10.1111/bmsp.12019>

McLachlan, G. J., Baek, J., and Rathnayake, S. I. (2011). "Mixtures of Factor Analyzers for the Analysis of High-Dimensional Data." *Mixtures: Estimation and Applications*, 189–212.

McLachlan, G. J., Peel, D., and Bean, R. (2003). "Modelling high-dimensional data by mixtures of factor analyzers." *Computational Statistics & Data Analysis*, 41(3): 379–388.

McNicholas, P. D. (2016). *Mixture model-based classification*. CRC Press.

McNicholas, P. D. and Murphy, T. B. (2008). "Parsimonious Gaussian mixture models." *Statistics and Computing*, 18(3): 285–296.

Meredith, M. and Kruschke, J. (2018). *HDInterval: Highest (Posterior) Density Intervals*. R package version 0.2.0.

URL <https://CRAN.R-project.org/package=HDInterval>

Murphy, K., Viroli, C., and Gormley, I. C. (2018). "Infinite Mixtures of Infinite Factor Analyzers." *Bayesian Anal.*. Advance publication.

URL <https://doi.org/10.1214/19-BA1179>

Muthén, L. and Muthén, B. (2019). "Mplus." *The comprehensive modelling program for applied researchers: user's guide*, 5.

Neudecker, H. (1981). "On the matrix formulation of Kaiser's varimax criterion." *Psychometrika*, 46(3): 343–345.

Papastamoulis, P. (2016). "label.switching: An R Package for Dealing with the Label Switching Problem in MCMC Outputs." *Journal of Statistical Software*, 69(1): 1–24.

— (2018). "Overfitting Bayesian mixtures of factor analyzers with an unknown number of components." *Computational Statistics & Data Analysis*, 124: 220–234.

— (2019). *fabMix: Overfitting Bayesian Mixtures of Factor Analyzers with Parsimonious Covariance and Unknown Number of Components*. R package version 5.0.

URL <http://CRAN.R-project.org/package=fabMix>

— (2020). "Clustering multivariate data using factor analytic Bayesian mixtures with an unknown number of components." *Statistics and Computing*, 30: 485–506.

Papastamoulis, P. and Iliopoulos, G. (2010). "An artificial allocations based solution to the label switching problem in Bayesian analysis of mixtures of distributions." *Journal of Computational and Graphical Statistics*, 19: 313–331.

Piatek, R. (2019). *BayesFM: Bayesian Inference for Factor Modeling*. R package version 0.1.3.

URL <https://CRAN.R-project.org/package=BayesFM>

R Core Team (2018). *R: A Language and Environment for Statistical Computing*. R Foundation for Statistical Computing, Vienna, Austria.

URL <https://www.R-project.org/>

Ročková, V. and George, E. I. (2016). "Fast Bayesian Factor Analysis via Automatic Rotations to Sparsity." *Journal of the American Statistical Association*, 111(516): 1608–1622.
URL <https://doi.org/10.1080/01621459.2015.1100620>

Rodriguez, C. and Walker, S. (2014). "Label switching in Bayesian mixture models: deterministic relabelling strategies." *Journal of Computational and Graphical Statistics*, 23(1): 25–45.

Romeo, F. and Sangiovanni-Vincentelli, A. (1991). "A theoretical framework for simulated annealing." *Algorithmica*, 6(1-6): 302.

Rosseel, Y. (2012). "lavaan: An R Package for Structural Equation Modeling." *Journal of Statistical Software*, 48(2): 1–36.
URL <http://www.jstatsoft.org/v48/i02/>

Schwarz, G. (1978). "Estimating the Dimension of a Model." *Ann. Statist.*, 6(2): 461–464.
URL <https://doi.org/10.1214/aos/1176344136>

Sherin, R. J. (1966). "A matrix formulation of Kaiser's varimax criterion." *Psychometrika*, 31(4): 535–538.

Snapper, E. (1979). "Characteristic polynomials of a permutation representation." *Journal of Combinatorial Theory, Series A*, 26(1): 65–81.

Song, X.-Y. and Lee, S.-Y. (2001). "Bayesian estimation and test for factor analysis model with continuous and polytomous data in several populations." *British Journal of Mathematical and Statistical Psychology*, 54(2): 237–263.

Stan Development Team (2019). "RStan: the R interface to Stan." R package version 2.19.2.
URL <http://mc-stan.org/>

Stephens, M. (2000). "Dealing with label switching in mixture models." *Journal of the Royal Statistical Society B*, 62(4): 795–809.

ten Berge, J. M. (1984). "A joint treatment of varimax rotation and the problem of diagonalizing symmetric matrices simultaneously in the least-squares sense." *Psychometrika*, 49(3): 347–358.

Thurstone, L. L. (1934). "The vectors of mind." *Psychological review*, 41(1): 1.

West, M. (2003). "Bayesian Factor Regression Models in the "Large p, Small n" Paradigm." In *Bayesian Statistics*, 723–732. Oxford University Press.

Appendix

A. Comparison of multiple chains

Running parallel chains is a standard practice in MCMC applications (see e.g. Carpenter et al., 2017) in order to assess convergence. Applying our method to each chain separately will make the factor loadings identifiable *within* each chain. However, the post-processed outputs will not be directly comparable *between* chains. Clearly, one run may be a signed permutation of another, provided that the chains have converged to their stationary distribution. Thus, it makes sense to post-process the chains in order to switch all of them in a same neighbourhood.

This reduces to find *a single* sign-permutation per chain that will reorder *all values* of the given chain. Let Λ_c^* denotes the Λ^* matrix (that is, the matrix which contains the estimates of posterior mean of factor loadings) for chain $c = 1, \dots, C$, where C denotes the total number of parallel chains. In order to find the final sign-permutations per chain we only have to apply Algorithm 1 on Λ_c^* , $c = 1, \dots, C$. Let now $\hat{\Lambda}^{(t,c)}$ denotes the (reordered) matrix of factor loadings for chain c on iteration t and $\hat{Q}^{(c)}$ the resulting sign-permutation for chain c . Then, the final step is to transform $\hat{\Lambda}^{(t,c)}$ to $\hat{\Lambda}^{(t,c)} \hat{Q}^{(c)}$, for all $t = 1, \dots, M$, $c = 1, \dots, C$.

We illustrate this procedure on the simulated dataset 1 (used in Section 4.1). We used Stan (Carpenter et al., 2017) in order to generate 8 chains of 10K iterations, following a burn-in period of 1000. Figure A.1 displays the raw and post-processed output from successive segments of each chain. The first segment displays the first 100 raw and post-processed iterations of the first chain, the second segment displays the raw and reordered values of iterations 101 – 200 for the second chain, and so on. The black coloured points correspond to successive segments of the simultaneously processed chains. It is evident that all chains have been successfully switched on a common labelling. Moreover, both the point estimate and the upper limit of the 95% confidence interval of the potential scale reduction factor (Gelman et al., 1992; Brooks and Gelman, 1998) are equal to 1.00 for all loadings, indicating that there are no convergence issues.

B. Computational benchmark: Performance comparison in high dimensional factor analytic models

Figure B.1 displays the progress of successive evaluations of the objective function (15) versus the time needed in order to reach the specific iteration of the algorithm. In all cases, the number of retained MCMC draws is equal to 10K, generated from Stan (following a burn-in period of 10K). Note that the time required in order to generate these MCMC samples with Stan ranges from a few minutes (for $q = 5, 10$) to five days (for $q = 50$).

In the partial simulated annealing scheme we used $B = 20$ simulated annealing steps/repetitions for $q = 5, 10$ factors and $B = 200$ for $q = 30, 50$ factors. In the full simulated annealing scheme we used $B = 100, 100, 500$ and 2000 simulated annealing

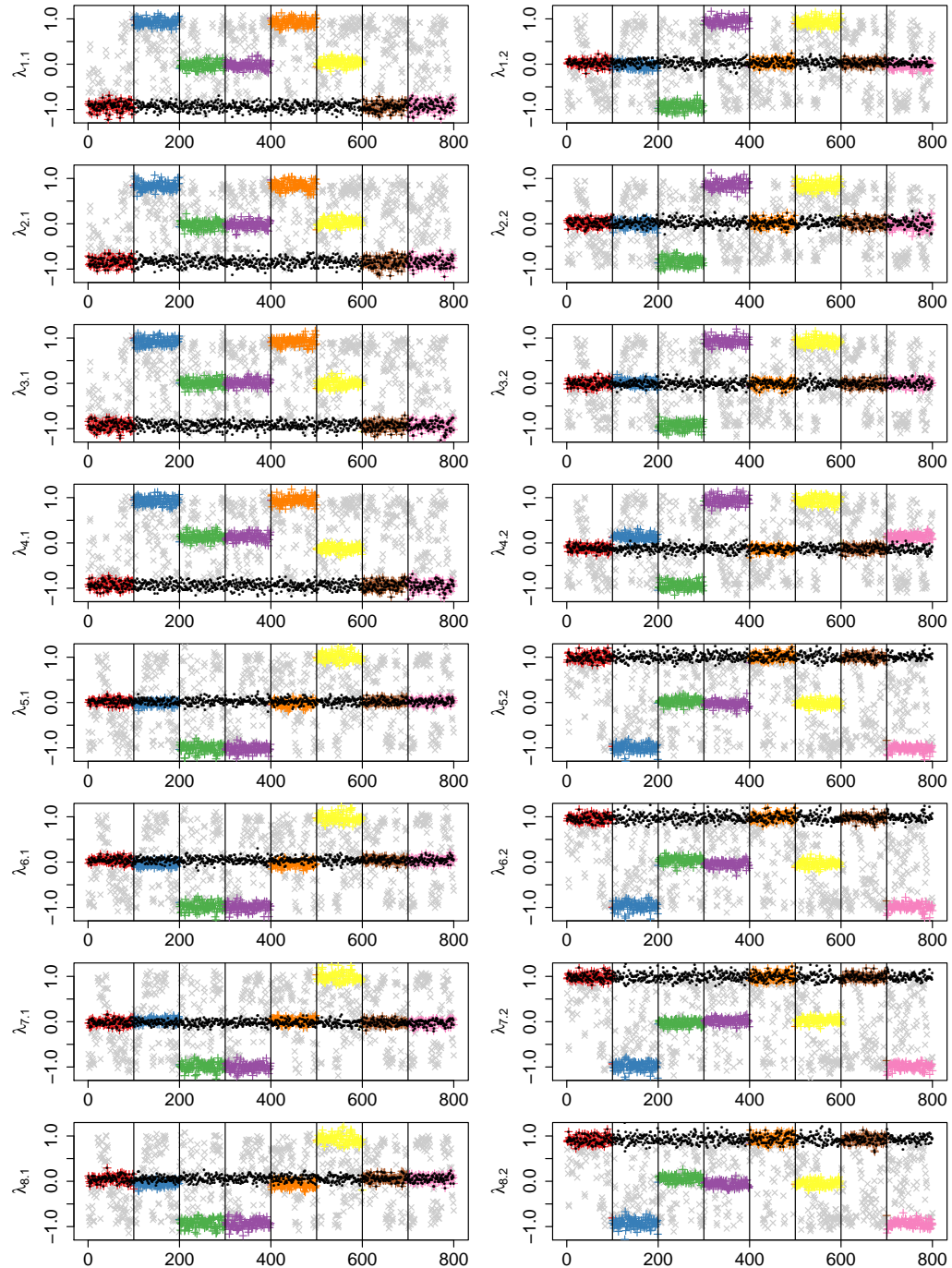


Figure A.1: Simulated data 1: Trace plots of the generated loadings before and after the implementation of RSP algorithm.

Notes: Gray-coloured points: raw output of factor loadings (8 parallel chains from Stan); Segments (vertical lines): 100 successive MCMC draws. Coloured points: RSP reordered factor loadings. Black trace: sign-permuted reordered traces making all chains comparable.

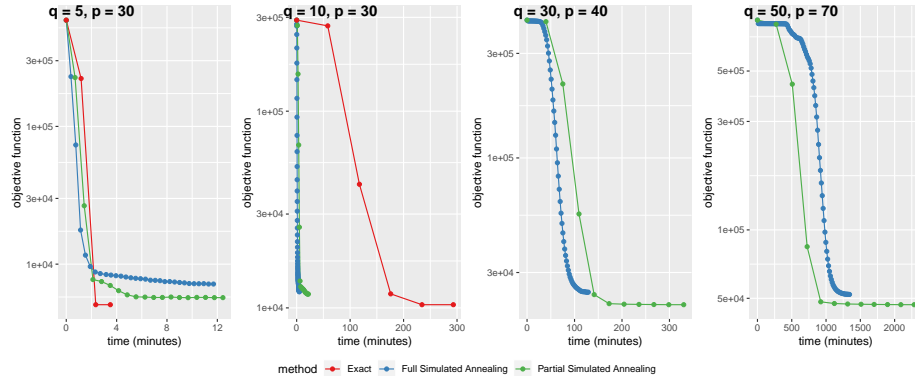


Figure B.1: Comparison of the three computational schemes into four datasets for various number of factors (q) and observed variables (p).

Notes: *Y axis: in log-scale. Exact version (Scheme A) is not applied for $q > 10$. MCMC details: 10K iterations using Stan.*

steps/repetitions for $q = 5, 10, 30$ and 50 factors, respectively. Observe that for typical values of the number of factors (e.g. $q = 5$) the exact scheme should be preferred. As expected, the partial simulated annealing scheme performs better than the full simulated scheme and should be preferred whenever the exact algorithm is large (e.g. when $q > 10$). At first, in all cases, the algorithm under the full simulated annealing scheme (blue line) converges to a worse (i.e., larger) value of the objective function compared to all other schemes. Second, observe that when the number of factors is larger than 10, the algorithm under the full simulated annealing scheme demands a large number of iterations in order to escape from the initial values and start the descend.

The post-processed values for the dataset with the 50 factors are presented in Figure B.2, which corresponds to the output returned by the partial simulated annealing algorithm. In this case, the number of factors used to generate the specific dataset is equal to 35, thus, when fitting a 50-factor model, there should be 15 redundant columns in the resulting matrix of factor loadings. A careful inspection of the 99% Highest Density Intervals (illustrated in blue) reveals that there are 15 panels where all intervals contain zero. The same holds for the 99% simultaneous Credible Region illustrated in red, that is, the panels corresponding to factor $j \in \{3, 10, 13, 14, 16, 17, 18, 22, 25, 26, 28, 31, 43, 45, 48\}$. The same holds for the 99% HDIs when using the full simulated annealing scheme (which converged to an inferior solution), but the 99% simultaneous credible region contain zero for 29 factors instead of 15 (results not shown).

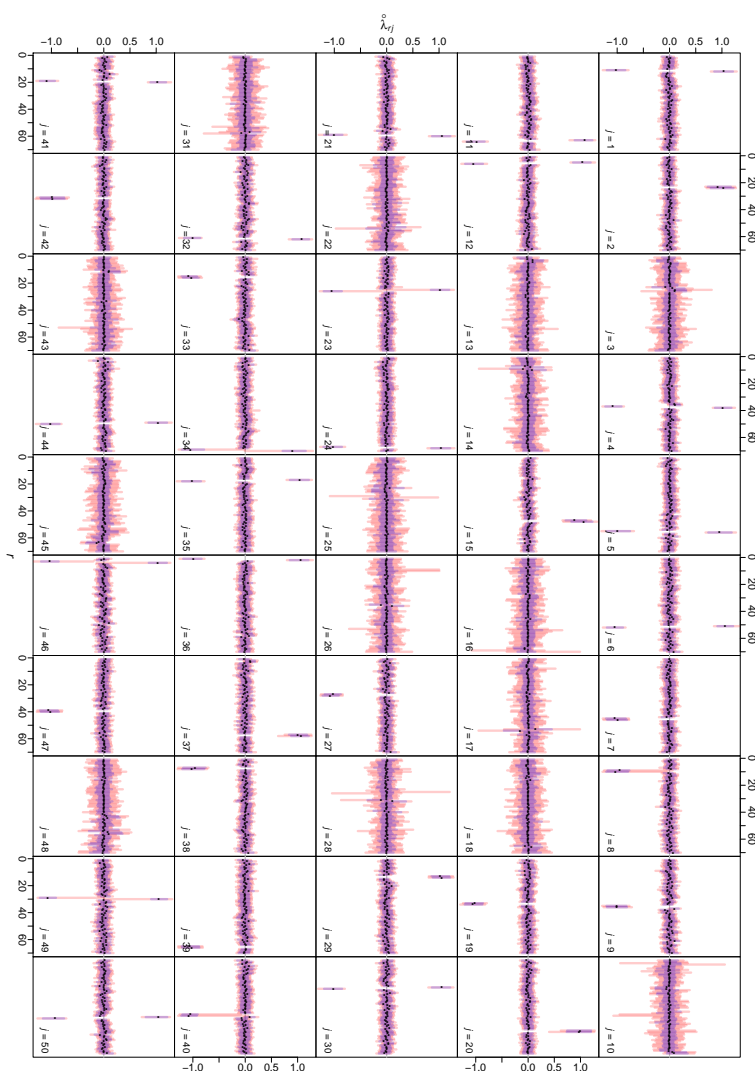


Figure B.2: Post-processed factor loadings according to RSP algorithm under the partial simulated annealing scheme, for a synthetic dataset of $n = 500$ observations and $p = 70$ variables.

Notes: *Fitted model*: $q = 50$ factors; *True factors*: $q_{true} = 35$. *Blue regions*: 99% Highest Density Intervals; *Red regions* : 99% Highest Density Intervals and *Simultaneous Credible Region Dots*: posterior means.

C. Mixtures of factor analyzers: The Wave dataset

We used the Wave dataset, available in the `fabMix` package in R. The dataset is generated from the Waveform Database Generator (Breiman et al., 1984) and consists of $p = 21$ variables, all of which include noise, and there are 3 underlying classes of waves. Papastamoulis (2018, 2020) fitted various parameterizations of the general model in Equation (17) assuming an unknown number of mixture components and using the Bayesian Information Criterion (Schwarz, 1978) for choosing q . The selected model corresponds to $K = 3$ clusters and $q = 1$ factors, under the constraint that $\Sigma_1 = \Sigma_2 = \Sigma_3$. The `fabMix` package (Papastamoulis, 2019) was used in order to produce a MCMC sample from the posterior distribution of the MFA model, using a prior parallel tempering scheme with 8 chains and a number of MCMC iterations equal to 20K. The clustered data as well as the inferred correlation matrix per cluster, conditional on $K = 3$ and $q = 1$, is shown in Figure C.1. The posterior means and 99% HDIs of the reordered factor loadings per cluster are presented in Figure C.2.

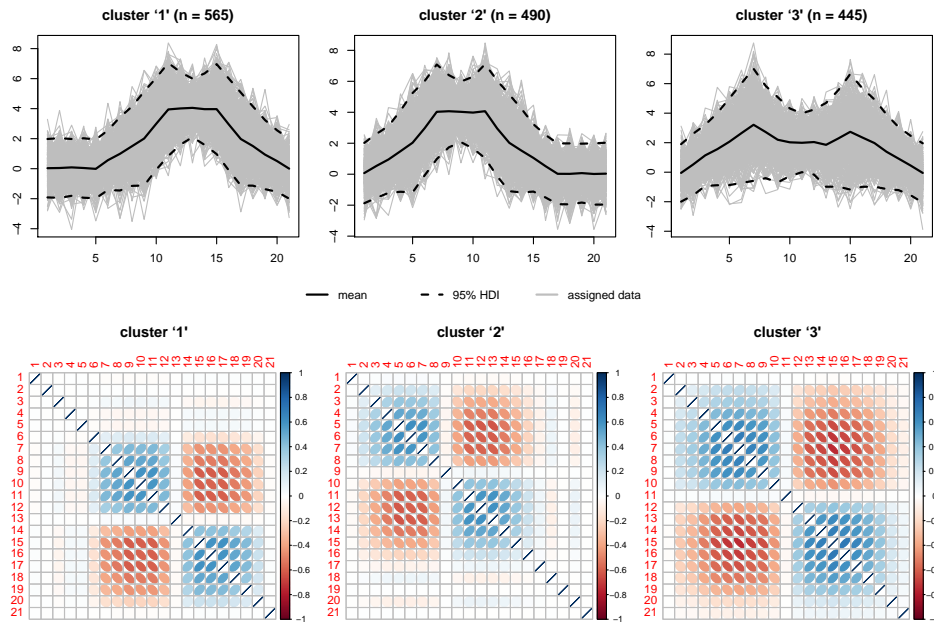


Figure C.1: *Wave dataset*: Assigned (21-dimensional) observations per cluster (1st row) and estimated correlation matrix per cluster (2nd row), according to a Bayesian mixture of factor analyzers with $K = 3$ clusters and $q = 1$ factors.

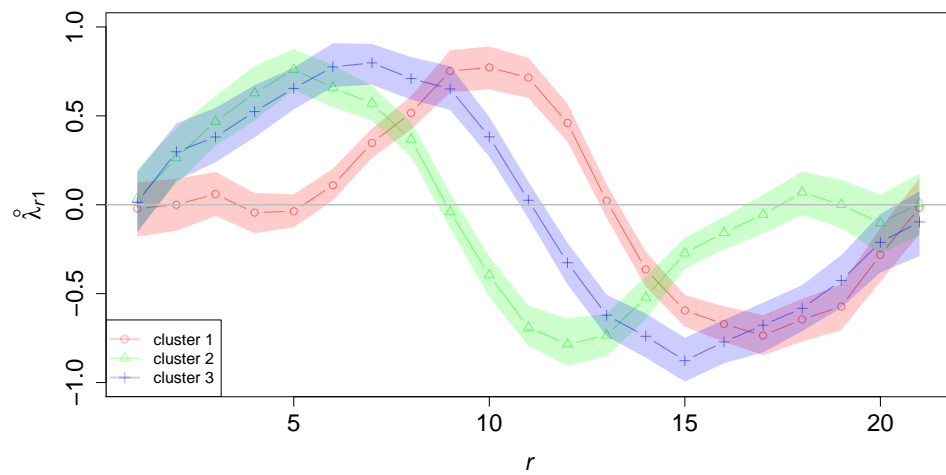


Figure C.2: *Wave dataset*: Posterior means and 99% HDIs for the reordered factor loadings per cluster.